DENDRITIC CELLS

Human lymphoid organ dendritic cell identity is predominantly dictated by ontogeny, not tissue microenvironment

Gordon F. Heidkamp,[1]* Jil Sander,[2]* Christian H. K. Lehmann,[1] Lukas Heger,[1] Nathalie Eissing,[1] Anna Baranska,[1†] Jennifer J. Lühr,[1] Alana Hoffmann,[1] Katharina C. Reimer,[1] Anja Lux,[3] Stephan Söder,[4] Arndt Hartmann,[4] Johannes Zenk,[5] Thomas Ulas,[2] Naomi McGovern,[6] Christoph Alexiou,[7] Bernd Spriewald,[8] Andreas Mackensen,[8] Gerold Schuler,[9] Burkhard Schauf,[10] Anja Forster,[10] Roland Repp,[11] Peter A. Fasching,[12] Ariawan Purbojo,[13] Robert Cesnjevar,[13] Evelyn Ullrich,[14,15] Florent Ginhoux,[6] Andreas Schlitzer,[2,6,16] Falk Nimmerjahn,[3] Joachim L. Schultze,[2,16]*‡ Diana Dudziak[1]*‡

In mice, conventional and plasmacytoid dendritic cells (DCs) derive from separate hematopoietic precursors before they migrate to peripheral tissues. Moreover, two classes of conventional DCs (cDC1 and cDC2 DCs) and one class of plasmacytoid DCs (pDCs) have been shown to be transcriptionally and functionally distinct entities. In humans, these three DC subtypes can be identified using the cell surface markers CD1c (cDC2), CD141 (cDC1), and CD303 (pDCs), albeit it remains elusive whether DC functionality is mainly determined by ontogeny or the tissue microenvironment. By phenotypic and transcriptional profiling of these three DC subtypes in different human tissues derived from a large number of human individuals, we demonstrate that DC subpopulations in organs of the lymphohematopoietic system (spleen, thymus, and blood) are strongly defined by ontogeny rather than by signals from the microenvironment. In contrast, DC subsets derived from human lung or skin differed substantially, strongly arguing that DCs react toward modulatory signals from tissue microenvironments. Collectively, the data obtained in this study may serve as a major resource to guide further studies into human DC biology during homeostasis and inflammation.

INTRODUCTION

Dendritic cells (DCs) are key players not only in the induction of adaptive immune responses against foreign pathogens but also in the maintenance of tolerance to innocuous host proteins (*1*–*4*). Distinct subsets of DCs have been defined on the basis of their ontogeny, functional properties, and phenotypic markers that allow one to distinguish DC subsets in both humans and animal models (*5*–*12*). In mice, DCs can be distinguished into plasmacytoid DCs (pDCs) and several lymphoid and nonlymphoid tissue-resident and tissue-migratory conventional DC subsets (*2*, *9*, *13*–*16*). Cross-presentation has been mainly associated with conventional DCs of type 1 (cDC1s, namely, CD8α^+ and CD103$^+$ DCs), albeit other DCs can also cross-present antigens, particularly under inflammatory conditions (*5*, *17*–*22*). Migration, expression of effector molecules, the presentation of antigens, and the induction of T cell activation by murine DC subsets have been extensively studied in the past decades, resulting in a rather sophisticated model describing DC biology in the context of immune activation, inflammation, and pathogenesis of many diseases. Murine DCs constitute a separate hematopoietic cell lineage (*8*, *10*, *12*, *15*) with postulated common precursors, including macrophage-DC precursor cells and common DC precursor cells (*2*, *7*, *9*, *10*, *12*, *15*, *23*). For both DC precursors and differentiated DC subsets, combinations of transcriptional regulators (TRs) involved in differentiation, cell type definition, or function were identified (*2*, *10*, *24*–*39*). For example, *Pu.1* is crucial for the development of all murine DC subpopulations; *E2-2* has been linked to the pDC subset; and *Irf8*, *Id2*, and *Batf3* seem to define CD8α^+ and CD103$^+$ DCs, whereas CD11b$^+$ DCs were found to depend on *Irf4*, *Relb*, and *Notch2* (*2*, *9*, *13*, *24*, *25*, *27*, *29*, *30*).

The expression of HLA-DR and the lack of lineage markers for T cells, B cells, or natural killer (NK) cells are common to the myeloid cell lineage, thus including all human DC subpopulations (*2*, *9*, *40*, *41*). Nevertheless, for a long time, interspecies comparisons of human and murine DC subsets were hampered by the lack of markers allowing for a comparable separation of DC subsets in both species. However, during the past years, most of the human equivalents of the murine DC subsets have been defined (*9*, *15*, *40*–*50*). CD303$^+$ (BDCA2) pDCs

[1]Department of Dermatology, Laboratory of Dendritic Cell Biology, Friedrich-Alexander University Erlangen-Nürnberg (FAU), University Hospital Erlangen, Erlangen, Germany. [2]LIMES (Life and Medical Sciences) Institute, Genomics and Immunoregulation, University of Bonn, Bonn, Germany. [3]Department of Biology, Chair of Genetics, FAU, Erlangen, Germany. [4]Department of Pathology, FAU, University Hospital Erlangen, Erlangen, Germany. [5]Department of Otorhinolaryngology, Klinikum Augsburg Süd, Augsburg, Germany. [6]Singapore Immunology Network, A*STAR (Agency for Science Technology and Research), Singapore, Singapore. [7]Section for Experimental Oncology and Nanomedicine, Department of Otorhinolaryngology, Head and Neck Surgery, Else Kröner-Fresenius-Stiftung-Professorship, FAU, University Hospital Erlangen, Erlangen, Germany. [8]Department of Medicine 5, Hematology and Oncology, FAU, University Hospital Erlangen, Erlangen, Germany. [9]Department of Dermatology, FAU, University Hospital Erlangen, Erlangen, Germany. [10]Department of Obstetrics and Gynecology, Sozialstiftung Bamberg, Bamberg, Germany. [11]Medical Department 2, Städtisches Krankenhaus Kiel, Kiel, Germany. [12]Department of Gynecology and Obstetrics, Comprehensive Cancer Center Erlangen-EMN, FAU, University Hospital Erlangen, Erlangen, Germany. [13]Department of Pediatric Cardiac Surgery, FAU, University Hospital Erlangen, Erlangen, Germany. [14]LOEWE Center for Cell and Gene Therapy, Goethe University, Frankfurt, Germany. [15]Division for Stem Cell Transplantation and Immunology, Department for Children and Adolescents Medicine, Hospital of the Goethe University, Frankfurt, Germany. [16]Platform for Single Cell Genomics and Epigenomics (PRECISE) at the University of Bonn and the German Center for Neurodegenerative Diseases, Bonn, Germany.
*These authors contributed equally to this work.
†Present address: Centre d'Immunologie de Marseille-Luminy, Aix Marseille Université, INSERM-CNRS, Marseille-Luminy, France.
‡Corresponding author. Email: diana.dudziak@uk-erlangen.de (D.D.); j.schultze@uni-bonn.de (J.L.S.)

share very similar phenotypes and functions with murine pDCs (*27*, *29*, *51*, *52*). Human CD1c$^+$ (BDCA1, cDC2) DCs may be the counterpart of murine cDC2 DCs, and CD141$^+$ (thrombopoietin, BDCA3, cDC1) DCs may be the equivalent of conventional murine cDC1 DCs (*14*–*16*, *40*, *44*, *45*, *48*, *50*). In addition to individual phenotypic markers and the functional characterization, DCs have been extensively studied by genome-wide assessment of transcriptional regulation (*53*). However, the large majority of previous studies on human DCs (i) addressed only the biology of in vitro generated monocyte-derived DCs, (ii) were derived before the definition of the three major DC subsets (CD303$^+$ pDCs, CD1c$^+$ DCs, and CD141$^+$ DCs), or (iii) assessed only one of these subsets. Only a small number of transcriptomic studies compared blood DC subsets to human skin, intestinal lamina propria, lymph node, or tonsil DC subsets, but DCs from other human tissues were not part of those reports (*40*, *50*, *54*–*56*).

In light of recent findings concerning the transcriptional plasticity within the monocyte and macrophage compartment (*57*–*59*), it remains to be answered whether such plasticity is also seen for human DC subsets derived from different tissues. By studying CD1c$^+$ and CD141$^+$ DCs, as well as CD303$^+$ pDCs in different lymphoid human organs, we provide evidence that human DC subsets in organs of the lymphohematopoietic system are mainly characterized by a subset-specific transcriptional program with only a minor contribution of tissue-derived signals to their overall functional phenotype. In contrast, DCs derived from tissues such as lung or skin differ substantially from blood-derived DC subsets.

RESULTS

Identification of DC subpopulations in different human lymphohematopoietic organs

To characterize human DC subpopulations in various lymphohematopoietic tissues, we prepared single-cell suspensions from tissue samples of healthy individuals. We first sought to elucidate the relative distribution of the three main DC subpopulations CD1c$^+$ and CD141$^+$ DCs, as well as pDCs, in comparison to CD14$^+$ monocytes/macrophages in the various human tissues via multicolor flow cytometry according to previous reports (*14*, *16*, *40*) (Fig. 1). After gating on living, single, nonautofluorescent, lineage-negative (Lin$^-$) HLA-DR$^+$ cells (fig. S1), we identified a varying percentage of the different DC subpopulations and monocytes/macrophages dependent on the analyzed tissue (Fig. 1, A to C, and table S1A). CD1c$^+$ DCs represented the most prominent DC subpopulation in the Lin$^-$HLA-DR$^+$ compartment in blood (2.14 ± 1.26%, 30 donors), spleen (5.4 ± 6.03%, 30 donors), bone marrow (1.7 ± 2.67%, 22 donors), and cord blood (12.9 ± 8.12%, 43 donors), whereas pDCs were the dominant population within thymus (19.45 ± 14.98%, 56 donors) and tonsils (15.8 ± 15.64%, 54 donors) of all Lin$^-$HLA-DR$^+$ cells. We found CD141$^+$ DCs as the population with the lowest frequencies within the Lin$^-$HLA-DR$^+$ cell fractions in all investigated organs with the exception of human spleen (3.7 ± 6.83%) (Fig. 1, B and C). In summary, our data indicate that the proportion of individual DC subpopulations is varying between the different lymphohematopoietic organs but is conserved between individuals.

To extend the knowledge of the expression profile of particular cell surface molecules already described for blood DCs, we performed parallel flow cytometry analyses using different organs (Fig. 1D). Despite the fact that SIRPA (CD172a), which is a common marker for the determination of murine CD11b$^+$ DCs, was expressed on all CD1c$^+$ DCs, we also found high expression levels on CD14$^+$ monocytes as well as on pDCs in the various tissues. Further along these lines, CD64 (FCGRI) is known as a macrophage marker, which we also found to be expressed on the CD1c$^+$ DCs in blood, spleen, thymus, tonsils, and bone marrow, albeit to a lower level compared with monocytes. In all tissues analyzed, we detected a unique expression of Clec9A on CD141$^+$ DCs, supporting the idea of Clec9A as a CD141$^+$ DC subset–specific marker (*47*). BDCA-4 (CD304), CCR7, and CD45RA were specifically present on steady-state pDCs, whereas the costimulatory molecule CD86, but not the activation marker CD83, was expressed on all DCs and monocytes in the different lymphohematopoietic organs.

DC subtype, not tissue of origin, is the major transcriptional classifier in the human DC continuum

To understand global differences and the impact of tissue localization, we performed whole transcriptome analyses on CD1c$^+$ DCs, CD141$^+$ DCs, and pDCs, each derived from blood, spleen, and thymus from up to three different individuals by high-purity cell sorting (table S2). In addition, CD14$^+$ monocytes, CD3$^+$CD4$^+$ and CD3$^+$CD8$^+$ T cells, and CD19$^+$/CD20$^+$ B cells were sorted from the same peripheral blood samples. From each of the 37 different samples, 10,000 cells were used for transcriptomic analysis (fig. S2). Data were normalized and genes expressed in at least one group (present probes) were used for further analysis, including complexity reduction by principal components analysis (PCA), self-organizing map (SOM) clustering, correlation heat maps, coexpression networks, and heat map visualization of the most variable genes within the data set (Fig. 2A and fig. S2A). As expected, reducing the complexity by PCA revealed B and T cells to be distinct from DCs and monocytes (fig. S2B). Coexpression network analysis precisely identified four separate clusters, namely, (i) B and T cells, (ii) pDCs, (iii) CD1c$^+$ and CD141$^+$ DCs, and (iv) CD14$^+$ monocytes (fig. S2C), which was further corroborated by Pearson correlation coefficient matrix analysis (fig. S2D) and SOM clustering (fig. S2E). Metadata such as gender (fig. S2F) and age (fig. S2G) did not show any impact on the data structure. By focusing on the DC compartment (Fig. 2, B to F), transcriptome analysis revealed several important points. PCA showed pDCs to be separated from CD1c$^+$ and CD141$^+$ DCs irrespective of tissue origin (Fig. 2B). However, we also identified concise differences between cells from different lymphohematopoietic organs (Fig. 2C), suggesting that both cell type and tissue localization contribute to the overall transcriptome of DCs. SOM clustering based on all expressed genes corroborated this hypothesis, because each of the DC subtypes showed a specific pattern of gene regulation (Fig. 2D), indicating a contribution of cell type and localization. Nevertheless, coexpression network analysis on all present genes supported a hierarchy, with differences between pDCs and the myeloid DCs being the most prominent (Fig. 2E). Within the myeloid DC cluster, CD1c$^+$ DCs and CD141$^+$ DCs were located according to tissue origin. We could further validate these data by hierarchical clustering of the 1000 most variable genes (Fig. 2F), again demonstrating that cell type is the most important denominator of differences within transcriptional programs in human DC subtypes derived from organs of the lymphohematopoietic system.

Definition of signature genes of human lymphohematopoietic DC subtypes

Because cell ontogeny and cell subtype mainly determined transcriptional regulation of pDCs, CD1c$^+$ DCs, and CD141$^+$ DCs in blood,

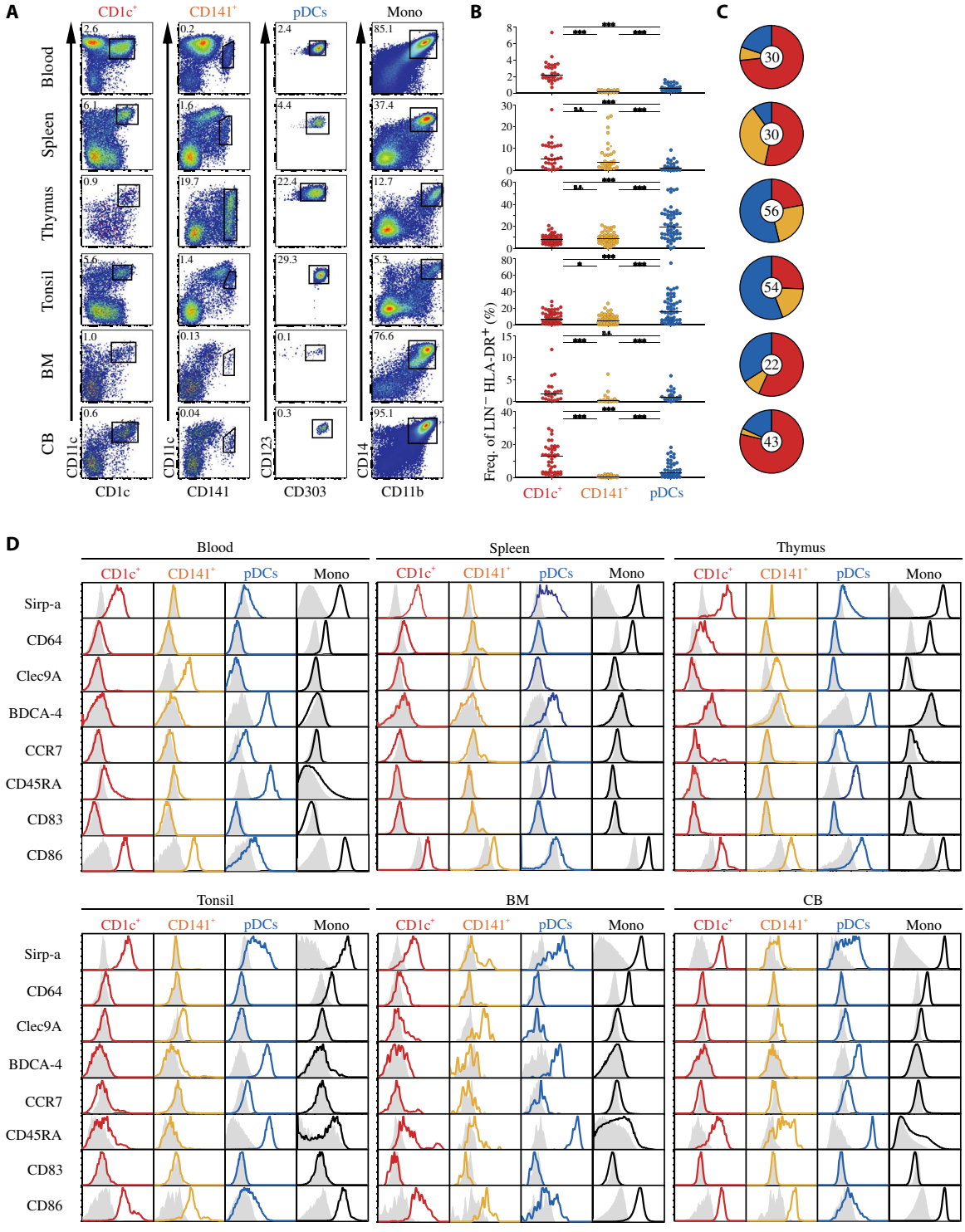

Fig. 1. Identification of DC subpopulations in different human lymphohematopoietic tissues. (**A**) Flow cytometric analysis of peripheral blood, spleen, thymus, tonsils, bone marrow (BM), and cord blood (CB). Tissue preparations were performed as described in Materials and Methods. Gating strategy was adapted from fig. S1 to display CD1c$^+$ DCs (red, CD1c$^+$CD11c^{high}), CD141$^+$ DCs (yellow, CD141$^+$CD11c^{int}), pDCs (blue, CD303$^+$CD123$^+$), and CD11b$^+$CD14$^+$ monocytes/macrophages (Mono) in the LIN$^-$(CD3$^-$CD19$^-$CD20$^-$CD56$^-$) HLA-DR$^+$ compartment. Numbers in each pseudo–color plot indicate frequencies of the respective DC subpopulation of LIN$^-$HLA-DR$^+$ cells. (**B**) Relative distributions of DC subpopulations within the LIN$^-$HLA-DR$^+$ compartment are summarized. Bars represent median distribution frequencies. Two-tailed Student's *t* test ($n \geq 30$) or Mann-Whitney *U* test ($n < 30$) was applied. ***$P < 0.001$, *$P < 0.05$; n.s., not significant $P \geq 0.05$. (**C**) Pie charts show the relative contribution of CD1c$^+$ DCs, CD141$^+$ DCs, and pDCs to the total DC pool in the respective organs. Numbers indicate donor counts analyzed. (**D**) Expression of typical DC or monocyte markers on cells from different lymphoid organs. Gating is based on fig. S1. Colored histograms display marker expression, and gray histograms display isotype controls. Representative data derived from at least five different donors per organ. Colors of gated cell populations are kept consistent throughout the article.

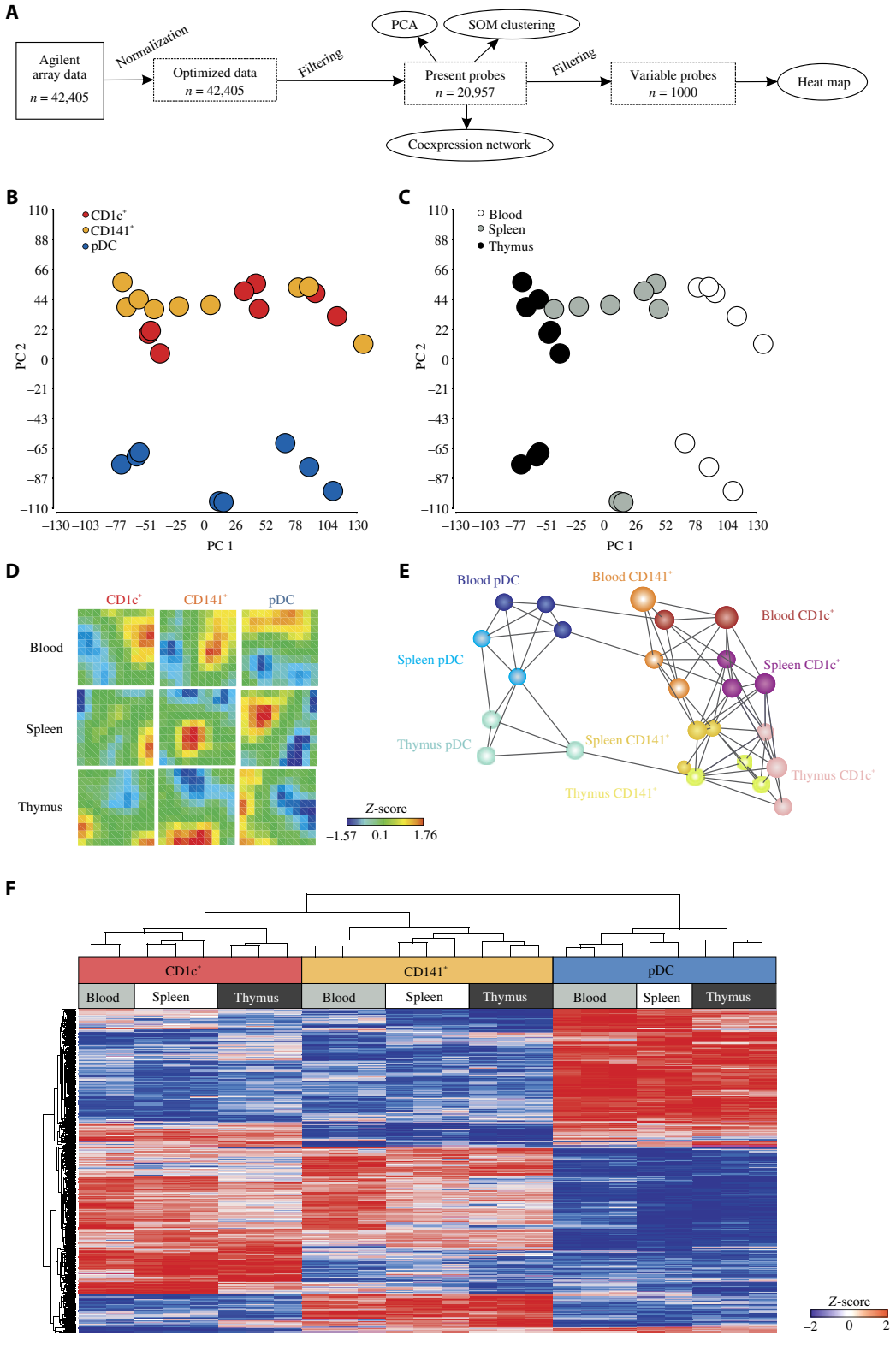

Fig. 2. Transcriptomic analysis of DC subsets in blood, spleen, and thymus. DC subpopulations from three donors of blood, splenic, or thymus tissue were sorted by flow cytometry, and whole human genome Agilent microarray analyses were performed. (**A**) Scheme describing the workflow. (**B** and **C**) PCAs (PC1 versus PC2) based on 20,957 present probes showing the distribution of samples according to (B) the DC subsets and (C) the organ. (**D**) SOM clustering based on present probes using 20,000 training iterations. (**E**) Coexpression network based on present probes. Two samples (nodes) are connected if the correlation score between their corresponding anti-$\log_2$ expression profiles is at least 0.97. (**F**) Hierarchical clustering based on the 1000 most variable probes across the data set. Log_2-transformed expression values were *z*-transformed and scaled to a minimum of –2 and a maximum of 2.

spleen, and thymus, we were next interested to determine DC subset–specific signature genes for these organs using linear support vector regression (SVR) (*60*) (fig. S3A). On the basis of the model described in Fig. 2, we predicted the largest number of signature genes for the determination of the three classes of DCs, followed by signature genes related to localization and the smallest number of signature genes for each cell type in its specific localization (Fig. 3, A to C, and table S3). We identified 76 signature genes for CD1c$^+$ DCs, 51 genes for CD141$^+$ DCs, and 117 genes for pDCs (Fig. 3A). The number of signature genes for DCs in a particular localization irrespective of DC subtype ranged from 17 (spleen) to 43 (thymus) (Fig. 3B), and signature genes for each cell type and localization ranged from 13 (pDCs in spleen) to 46 (CD1c$^+$ DCs in thymus) (Fig. 3C). To illustrate expression differences for individual examples of signature genes, we ranked them by expression level and differential expression with respect to other DC subtypes (table S3) and displayed absolute expression values as bar plots (Fig. 3, D to F, and fig. S3, B to D). Several immunoregulatory genes were found to be expressed only in one DC subtype; for example, *CLEC10A* (*CD301a*), *VEGFA*, and *FCGR2A* (*CD32A*) were only identified on all CD1c$^+$ DCs (Fig. 3D and fig. S3B), whereas *CLEC9A*, *IDO1*, and *XCR1* (*CCXCR1*) were only found on all CD141$^+$ DCs (Fig. 3D and fig. S3B). All pDCs were characterized by the expression of *FAM129C*, *CUX2*, and *GZMB* (Fig. 3D and fig. S3B). Whereas *GZMB* expression in pDCs has been previously reported (*61*), the roles of *FAM129C* and *CUX2* in pDCs remain elusive. *CLEC7A*, *C17orf87*, and *ARRB1* were expressed in all CD1c$^+$ and CD141$^+$ DCs but not in pDCs (fig. S3C). We also identified genes that were expressed in all DC types derived from a particular organ; for example, *SCAPER* and *MAN1B1-AS1* were expressed in all DCs derived from peripheral blood (Fig. 3E and fig. S3D), *HSPB1* and *BU963192* were expressed in DCs derived from spleen, and *USP41* and *TRBC2* were expressed in DCs from thymus (Fig. 3E and fig. S3D). Moreover, for each DC subtype within blood, spleen, or thymus, we could also identify genes specifically expressed in only one organ (Fig. 3F). Collectively, we identified numerous genes that can be used to distinguish different steady-state human DC subtypes across different lymphohematopoietic organs.

Identification of specific surface proteins distinguishing human lymphohematopoietic DC subtypes

Next, we aimed to identify genes encoding for cell surface proteins that could be used to distinguish the DC subpopulations at different localizations. We therefore determined the expression of up to 223 cell surface proteins on CD1c$^+$ DCs, CD141$^+$ DCs, and pDCs from blood, spleen, and thymus using a Lyoplate assay (Fig. 4, fig. S4, and table S4). Following an algorithm depicted in Fig. 4A, we focused on genes that showed differential expression on both mRNA and protein levels. Irrespective of localization, seven cell surface proteins were found on CD1c$^+$ DCs (TLR2, CD63, CD86, CD97, ITGAM, FCGR1, and IFNGR1) but not on CD141$^+$ DCs or pDCs (Fig. 4B). DPP4, ANPEP, and CD226 distinguish CD141$^+$ DCs from CD1c$^+$ DCs and pDCs. Furthermore, LAIR4 (CD305) and CXCR4 (CD184) are solely expressed on pDCs. When assessing marker genes for localization, only CD44 was shown to be expressed in all DCs in blood, and CD55 was shown to be expressed in all DCs derived from thymus (Fig. 4C). Similarly rare were markers identified on an individual subtype at a specific localization (Fig. 4D). Only for pDCs in thymus could we identify several genes, including CD47, TFRC, CD36, and CD7. Results of other surface proteins are summarized in fig. S4 and table S4. Collectively, we identified a decisive set of surface markers that can be used in combination with CD1c, CD141, and CD303/CD123 to distinguish human DC subsets in different lymphohematopoietic organs.

Identification of cell type– and tissue-associated gene modules

Further, we wanted to determine specific gene modules either associated with DC subtype or localization. Gene modules were defined on the basis of coexpression (*62*) and visualized as a network focusing on 452 signature genes previously identified in the data set (Fig. 5 and fig. S5). The topology of this network exhibited seven major clusters (C1 to C7, table S5). For each of the three DC subsets from blood, spleen, and thymus, we mapped differential gene expression against the overall mean onto the network, with genes enriched in the respective cell type displayed in red; for example, CD1c$^+$ DCs in peripheral blood showed elevated expression of genes in clusters C5 and C6 (Fig. 5A). Elevated expression of genes in cluster C5 was found in CD1c$^+$ DCs at all sites, suggesting that this cluster represented the CD1c$^+$ DC–specific co-regulated genes irrespective of localization (Fig. 5, A, D, and G). Cluster C2 harbored CD141$^+$ DC–specific genes (Fig. 5, B, E, and H), and pDC-specific genes were defined by cluster C7 (Fig. 5, C, F, and I). We also identified genes induced in all DC subtypes in blood (harbored in C6), spleen (C4), or thymus (C3). Network analysis also validated the hallmark genes defined by linear SVR analysis (Fig. 3); for example the pDC-related genes *FAM129C*, *CUX2*, and *GZMB* were central to the pDC-defining cluster C7. Other hallmark genes are also displayed in Fig. 5.

TRs of human lymphohematopoietic CD1c$^+$ DCs, CD141$^+$ DCs, and pDCs

The modular structure within the network allowed us to predict potential TRs upstream of coexpressed genes (Fig. 6). We developed an integrated approach (Fig. 6A) to identify groups of TRs that are related to the three different DC subsets. As a first step, we filtered the list of present genes for known TRs, which were further filtered by differential expression between the three DC subsets and further enriched for TRs previously linked to DC function (*10*, *16*, *25*, *27*, *28*). These candidate TRs were interrogated for binding prediction to the gene loci of the subtype-specific gene sets described in Fig. 5 (cluster C7 for pDCs, cluster C2 for CD141$^+$ DCs, and cluster C5 for CD1c$^+$ DCs), followed by an integrated ranking approach (table S6). TRs were subdivided into five categories, and normalized expression was plotted for each cell type separately (Fig. 6, B to D). For example, the TRs *CEBPB*, *SPI1*, *RUNX3*, *NFKB1*, and *BHLHE40* were among the top-ranked TRs in CD1c$^+$ DCs (Fig. 6B), and this subset was further characterized by diminished expression and binding prediction of *IRF8*, *MEIS1*, *NR5A1*, *TEAD2*, and *NFAT5*. The TRs *TEAD4*, *MYC*, and *TCF7L2* were among the top-ranked TRs in CD141$^+$ DC (Fig. 6C), whereas *ETS1*, *ARID3A*, *FOXM1*, and *TCF3* were among those TRs characterizing human pDCs (Fig. 6D).

To further corroborate these findings, we generated a coexpression analysis (CEA) network of the 558 TRs themselves (Fig. 6, E and F, and fig. S6). The topology of this network showed a circular structure with genes elevated in CD1c$^+$ and CD141$^+$ DCs located mainly on the right side, whereas pDC TRs were mainly elevated on the left side of the circle (fig. S6). Accordingly, by mapping the top-ranked TRs onto the TR network as determined and visualized in Fig. 6 (A to D), a larger cluster of pDC-related TRs was found to be located on the left side and a smaller CD1c$^+$ DC-related cluster was found to be located on the top right, but a specific CD141$^+$ DC–related cluster was not apparent

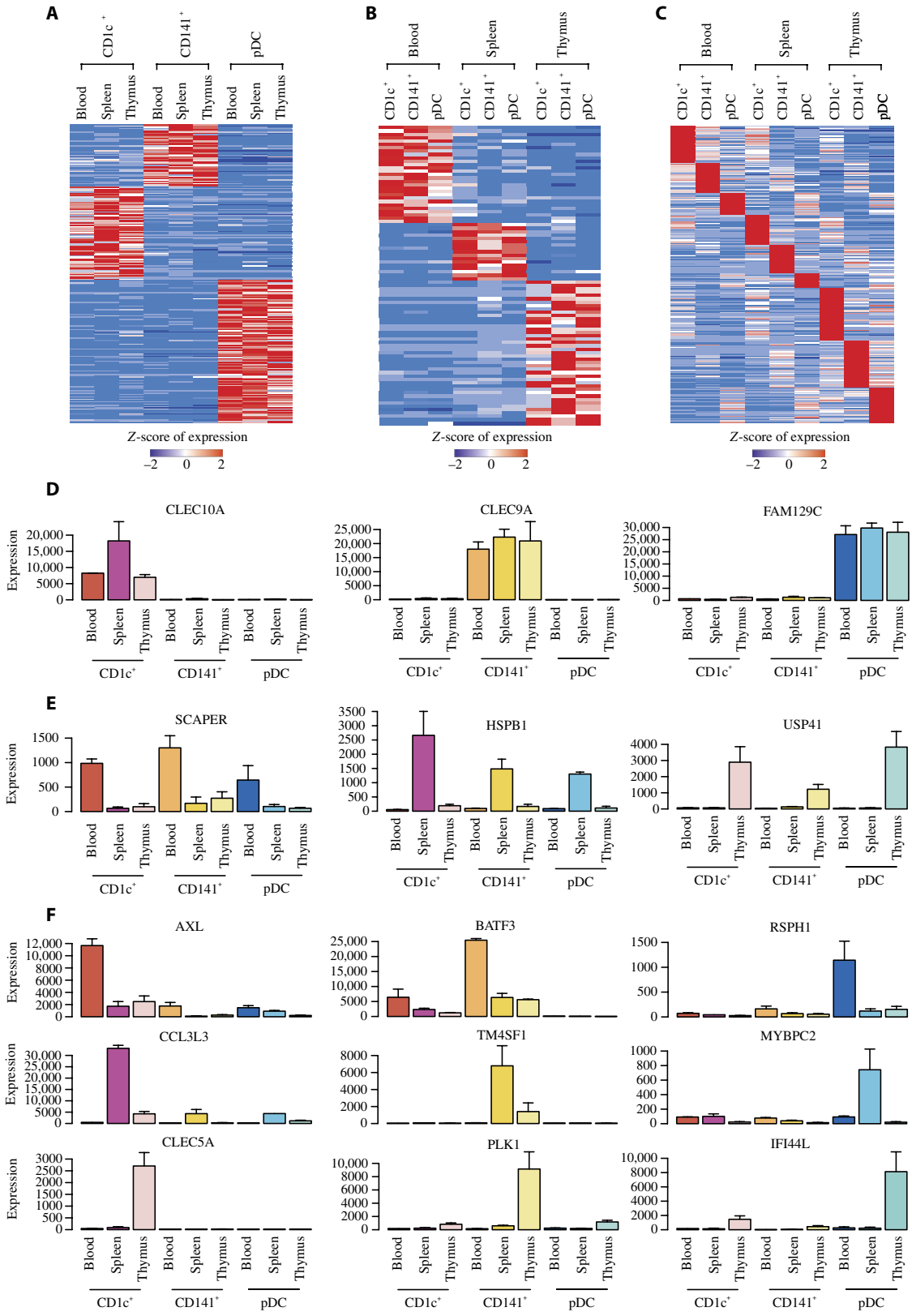

Fig. 3. Identification of signature and marker genes for human lymphohematopoietic DC subsets. (**A** to **C**) Heat maps of genes defined by linear SVR analysis being specific for (A) a particular DC subset irrespective of localization, (B) a particular organ, or (C) a single DC subset at a particular localization. Expression values were *z*-transformed and then scaled to a minimum of −2 and a maximum of 2. (**D** to **F**) Bar plots of marker candidates being specific for (D) a particular DC subset irrespective of localization, (E) a particular organ, or (F) a single DC subset in a particular localization.

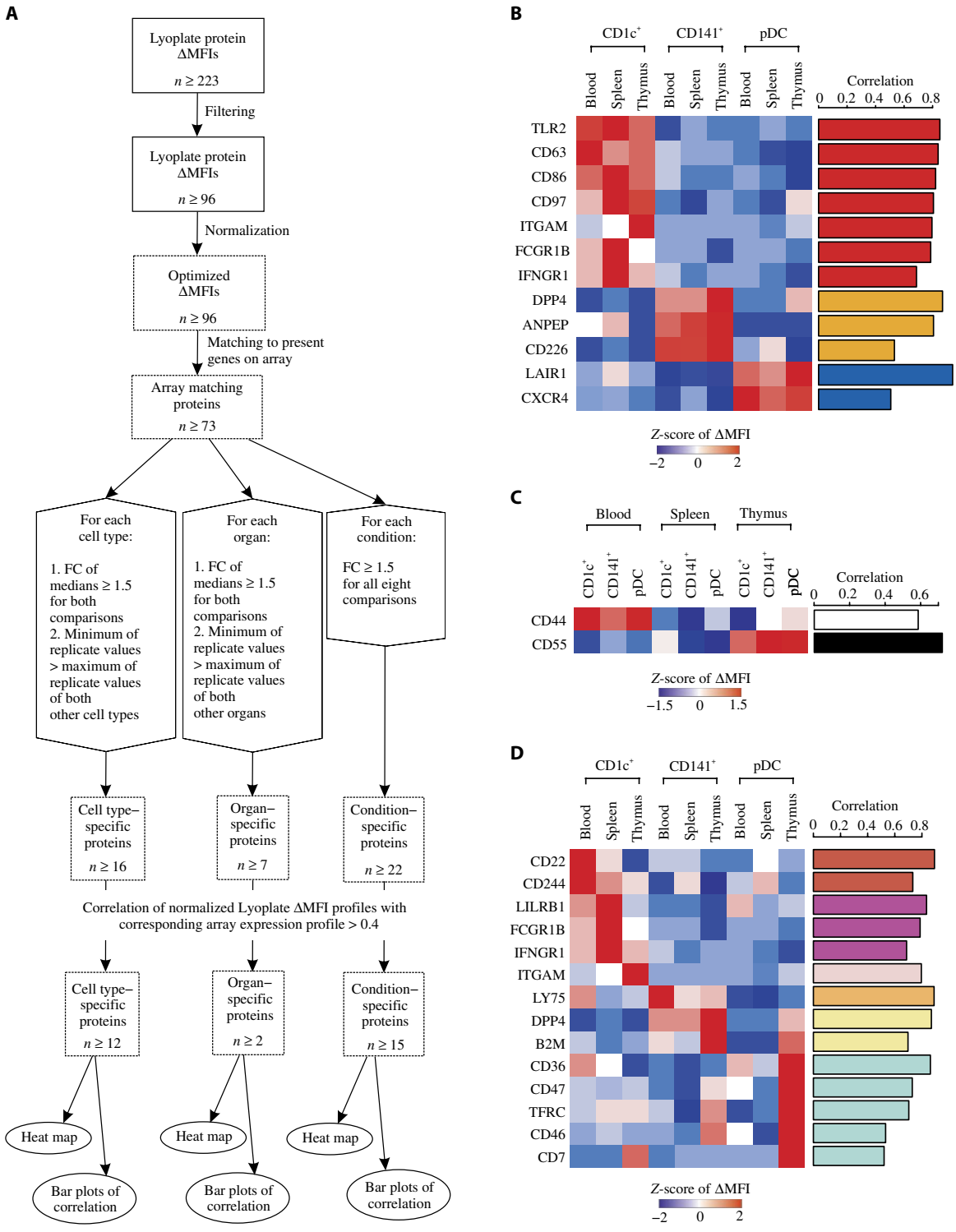

Fig. 4. Lyoplate analysis of cell surface markers on human lymphohematopoietic DC subsets. (**A**) Workflow. FC, fold change. (**B** to **D**) Heat maps of median fluorescence intensities (ΔMFIs) of cell surface markers determined by the workflow for (B) a particular DC subset irrespective of its localization, (C) a particular organ, or (D) a single DC subset at a particular localization. ΔMFI values were *z*-transformed and scaled to a minimum of −1.5 or −2 and a maximum of 1.5 or 2, respectively. Additionally, bar plots next to the heat maps display the correlation of each protein ΔMFI with the corresponding gene expression value on the microarray. Data are representative of two to three replicates using different donors.

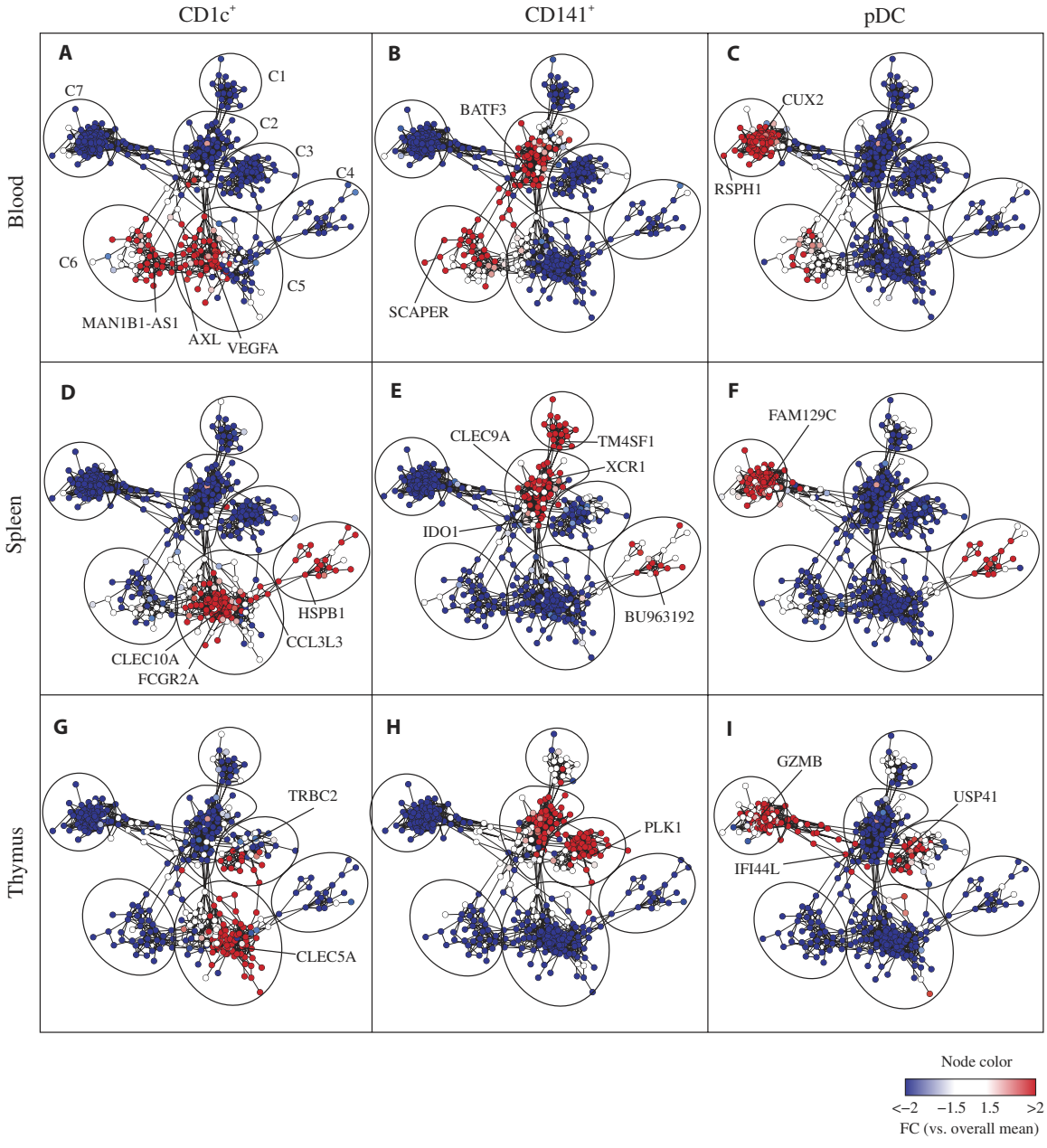

Fig. 5. Coexpression networks of signature genes in human lymphohematopoietic DC subpopulations. Coexpression networks of 452 genes identified as the union of signature genes defined by linear SVR. Only genes reaching a correlation cutoff of at least 0.8 are included in the network. (**A** to **I**) For each of the three DC subsets in the three different organs, the differential expression of the corresponding condition compared to the overall mean was mapped onto the network. Node colors range from blue (fold change ≤ −1.5) to red (fold change ≥ 1.5). Genes displayed in Fig. 3 (D to F) and fig. S3 (B to D) are highlighted if present in the network.

(Fig. 6E). When focusing on the top TRs being diminished in a particular DC subtype, we observed the opposite picture for pDCs, which were characterized by a diminished expression of many of the TRs elevated in CD1c$^+$ and/or CD141$^+$ DCs (Fig. 6F). There was a smaller cluster for diminished TRs in CD141$^+$ DCs, whereas no cluster structure among the top-ranked TRs in CD1c$^+$ DCs was found (Fig. 6F). Together, CEA not only validated the hallmark genes defined by linear SVR analysis but also allowed us to predict the potential TRs responsible for the respective cell type–specific transcriptional programs. Although localization showed an influence on TR expression, the major differences were again seen between the three different subtypes, particularly between pDCs and conventional DCs, whereas the difference between CD1c$^+$ and CD141$^+$ DC was not as prominent, reflecting their close relationship.

Transcriptional programs of DC subtypes in lung and skin are distinct

To determine the cellular relationship of DC subsets in non-lymphohematopoietic organs, we built upon a previous data set on skin and blood DCs (*40*), which did not contain data on Langerhans

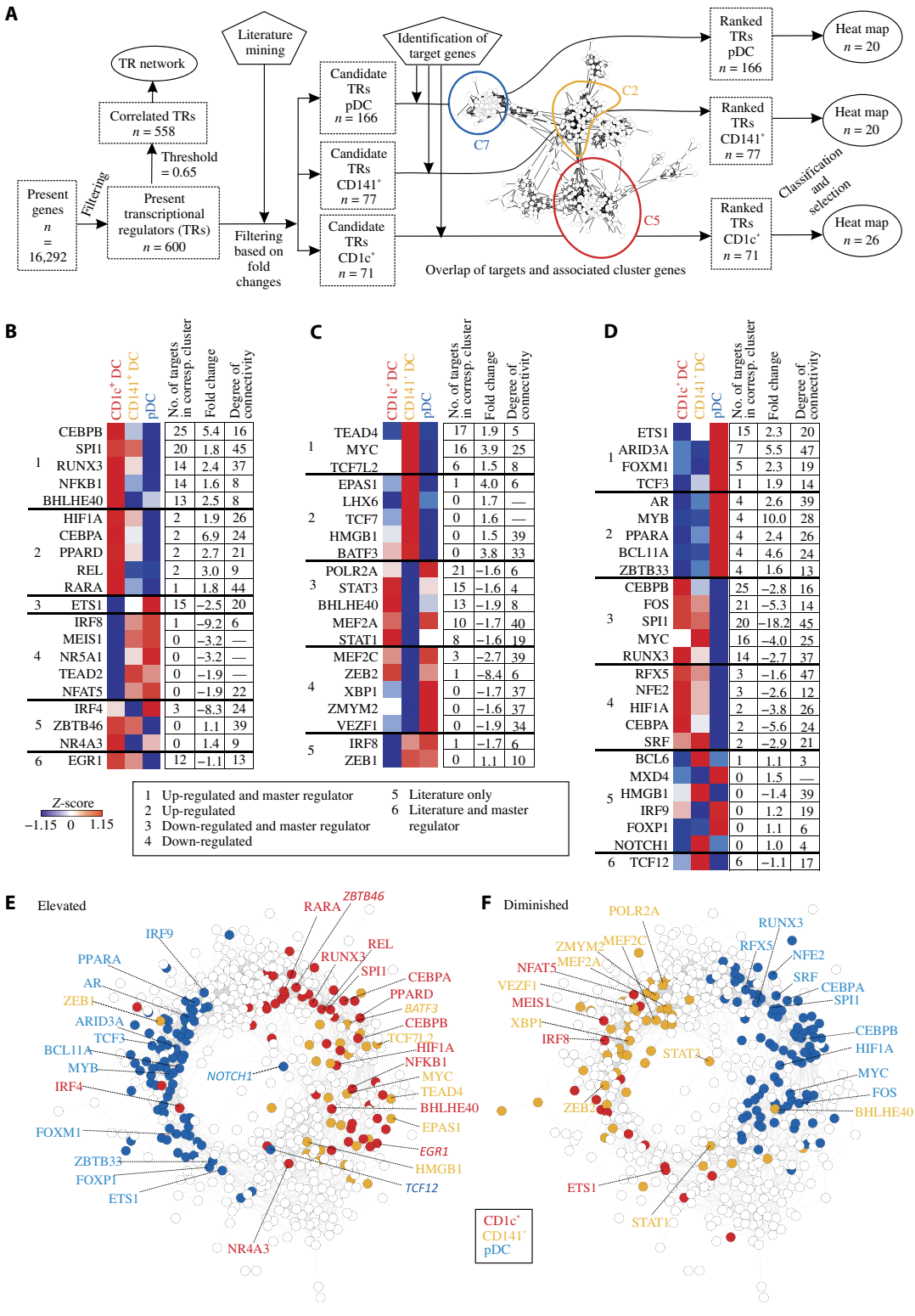

Fig. 6. TR networks of human DC subpopulations. (**A**) Workflow for this figure and fig. S6. (**B** to **D**) Heat maps of regulators being specifically linked to (B) CD1c$^+$ DCs, (C) CD141$^+$ DCs, or (D) pDCs on a transcriptional level. Log_2 expression values were *z*-transformed and scaled to a minimum of −1.15 and a maximum of 1.15, respectively. The regulators were grouped into six classes based on differential expression, literature-based knowledge, the overlap of predicted targets with genes of associated clusters (Fig. 5), and the degree of connectivity in the TR network. The top five ranked candidates for each class are displayed. If the class size was equal to 6 or smaller than 5, all candidates are displayed. Fold changes displayed next to the heat maps are the minimum of the twofold changes comparing the DC subpopulation of interest with the other ones, together with its sign (+ or –) of direction. (**E** and **F**) Coexpression networks of 558 TRs reaching a correlation cutoff of 0.65. The up-regulated (E) or down-regulated (F) candidates shown in (B) to (D) for CD1c$^+$ DCs (red), CD141$^+$ DCs (orange), and pDCs (blue) are highlighted. Regulators identified exclusively on the basis of literature mining are marked in italics.

cells, and extended this data set with DCs derived from human lung. For comparison with our data set of DCs derived from spleen, thymus, and blood, we developed an approach (Fig. 7A, fig. S7A, and Supplementary Materials) that allowed us to further assess genes interrogated in both studies (Fig. 7A and fig. S7B). Most of the differentially expressed genes showed similar behavior in both data sets (fig. S7C). For relationship analysis, we used Pearson correlation values as well as Euclidean distances between the subsets based on different sets of genes and performed hierarchical clustering on the obtained values (Fig. 7A). With only a small set of most differentially expressed genes, lymphohematopoietic CD1c$^+$ DC, CD141$^+$ DC, and pDC subsets were most closely related to each other irrespective of tissue origin (Fig. 7B and table S7). When comparing DC subsets from blood, skin, and lung, all DC subsets from one organ were more similar than the same subset from another tissue (Fig. 7C and table S7), indicating that transcriptional programs in DC subsets in non-lymphohematopoietic tissues are strongly influenced by tissue-derived signals. Nevertheless, when correlating a particular DC subset, for example, CD1c$^+$ DCs from the skin, these cells showed the highest correlation to CD1c$^+$ DCs from the other tissues (black squares), and the same was true for the other DC subsets, indicating that albeit tissue has a strong influence on transcriptional regulation of DCs in non-lymphohematopoietic tissues, ontogeny is still a major part of the transcriptional program. When extending the analysis to the 1000 genes with the highest variance in the data set (Fig. 7, D and E, and table S7), we obtained similar results, and even when using all present genes, pDCs were still separated from conventional DCs in lymphohematopoietic tissues (Fig. 7F and table S7), whereas this was not the case for non-lymphohematopoietic tissues (Fig. 7G and table S7). When using Euclidean distances, we obtained similar results (fig. S7, D to G). Collectively, DC subsets in lymphohematopoietic tissues are mainly determined by ontogeny, whereas DCs in tissues integrate additional tissue-derived signals, yet ontogeny remains an important driver of non-lymphohematopoietic tissue DC identity.

Linking human DC transcriptomes to previous knowledge

To put our data into context of previous findings, we performed gene set enrichment analysis (GSEA) using more than 10,000 gene sets in Molecular Signatures Database (MSigDB) (*63*), including the 5000 most recently published immune signatures, and plotted the top enriched signatures as BubbleMaps (*64*) (Fig. 8, fig. S8, and table S8). When comparing CD1c$^+$ and CD141$^+$ DCs, gene signatures derived from human myeloid cells compared to either B cells, T cells, or pDCs were apparent in CD1c$^+$ DCs (Fig. 8B), which at least in part might be due to a better coverage of this DC subset in previous studies because of their higher frequencies in tissues such as blood. In contrast, CD141$^+$ DCs showed enrichment of signatures derived from murine B cells and CD8$^+$ T cells, which most likely reflects the lack of signatures derived from these less frequent DCs in previous data sets. When comparing pDCs with either CD1c$^+$ or CD141$^+$ DCs, the top-ranked signatures were derived from comparisons of human pDCs to either monocytes, monocyte-derived DCs, or B cells. Similarly, when using Gene Ontology– and pathway-defined gene signatures from MSigDB, enrichment of a larger number of immune-related terms was observed for CD1c$^+$ DCs and pDCs, whereas only very few signatures were enriched in CD141$^+$ DCs (table S8), further indicating that the biology of these less frequent DCs is not yet sufficiently reflected in previous data.

To determine the relationship of DC subsets derived from lymphohematopoietic organs with the corresponding DC subsets from non-lymphohematopoietic tissues, we generated an additional 50 gene signatures derived from the most recent report on human and murine DC subsets by Haniffa *et al.* (*40*) extended with the DCs derived from human lung (Fig. 8C and table S8). In line with our own comparison between blood-, spleen-, and thymus-derived DC subsets, lung-derived pDCs were most closely related to pDCs from the other organs, and this was similarly true for lung and skin CD1c$^+$ and CD141$^+$ DCs (Fig. 8C).

Collectively, these data demonstrate that DC subpopulations in organs of the lymphohematopoietic system are mainly defined by ontogeny, whereas DC subsets derived from non-lymphohematopoietic human tissues, such as the lung or skin, are more strongly influenced by signals derived from their respective tissue microenvironments.

DISCUSSION

Here, we provide a comprehensive assessment of the overall distribution of the three major DC subpopulations in more than 235 human individuals in six lymphohematopoietic organs, including blood, spleen, thymus, tonsil, bone marrow, and cord blood. Although there is inter-individual variation, we observed tissue-specific distributions with highest frequencies of CD1c$^+$ DCs in blood, spleen, bone marrow, and cord blood; CD141$^+$ DCs in spleen; and pDCs in thymus and tonsils. Comparative analysis of genome-wide transcriptional regulation revealed that corresponding DC subsets derived from different lymphohematopoietic tissues (e.g., blood, thymic, and splenic pDCs) were most closely related, whereas tissue environment had less influence on the overall gene expression. However, when comparing blood-derived DCs as an example of a lymphohematopoietic tissue with DC subsets derived from other organs such as skin or lung, we revealed that signals from the tissue microenvironment of such organs have a much stronger impact on overall transcriptional regulation of DC subsets. This seems to be similar to monocytes and tissue macrophages that are characterized by very strong influences of the tissue microenvironment on the overall gene expression (*58*, *59*). Combining the assessment of more than 200 cell surface protein markers with global gene expression allowed us to define a set of marker genes that can be used to characterize the three DC subpopulations across tissues. CEA combined with network visualization revealed sets of genes specifically enriched in either pDCs, CD1c$^+$ DCs, or CD141$^+$ DCs. This information could be used to enrich prediction models for transcription factor networks associated with the three DC subsets. Determining the content of previously established knowledge in our human DC data set by applying more than 10,000 previously reported gene signatures indicated that the less frequent CD141$^+$ DCs are not sufficiently represented. We therefore propose a simple and straightforward approach to using gene signatures from newly found cell subsets and integrate these gene signatures into data depositories such as MSigDB (*63*, *65*).

Reliable cell surface markers are critical to properly identify and isolate different human DC subsets. In accordance with previous reports and our findings in this study, we suggest not to use single markers, but rather combinations such as CD123 and CD303 for pDCs, CD1c and CLEC10A for CD1c$^+$ DCs, and CD141 and CLEC9A for CD141$^+$ DCs in combination with HLA-DR, CD11c, CD11b, CD14, and a lineage cocktail to exclude T, B, and NK cells (*14*, *16*, *40*, *44*, *45*, *50*, *54*–*56*, *66*). Furthermore, CLEC10A- and CLEC9A-specific expression on the different DC subpopulations seems to be conserved between species, as revealed by the comparison to the ImmGen database of murine DCs (*10*). Therefore, according to our findings in up to six human lymphohematopoietic tissues, we postulate that these markers can be used to define the three major DC subpopulations in other organs as well.

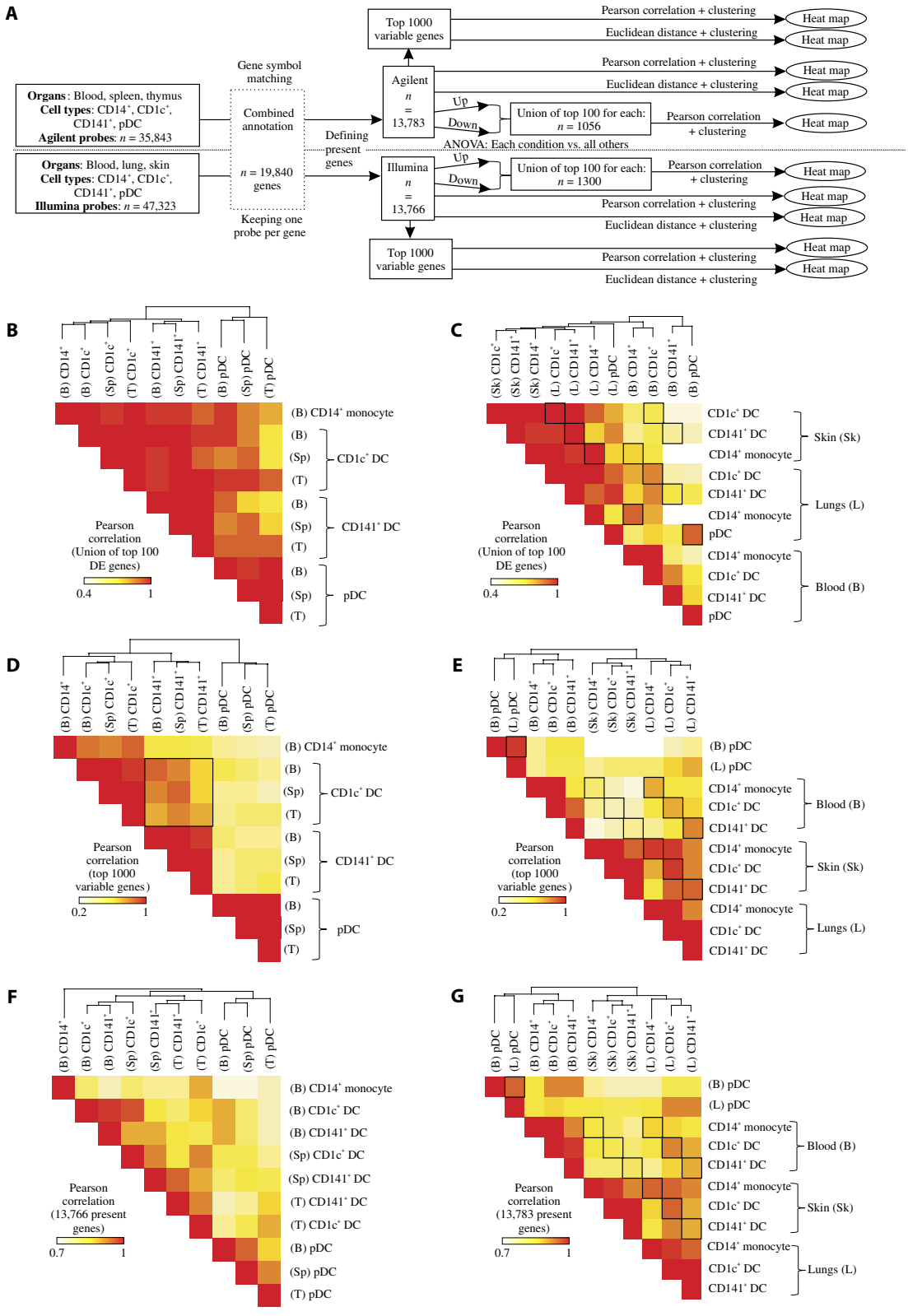

Fig. 7. Comparative analyses of different human lymphohematopoietic and non-lymphohematopoietic tissue DC transcriptional data sets. (**A**) Workflow. ANOVA, analysis of variance. (**B** to **G**) Pearson correlation values calculated pairwise between all cell types on the basis of either the union of the top 100 most differentially expressed genes (B and C), the top 1000 most variable genes (D and E), or present genes (F and G) for the data set with DC subsets from blood, spleen (Sp), or thymus (T) (B, D, and F) and the data set with DC subsets from blood, skin, and lung (C, E, and G). The results are displayed in the form of a heat map, where the color scaling ranges from white (low correlation) via yellow to red (high correlation). DE, differentially expressed.

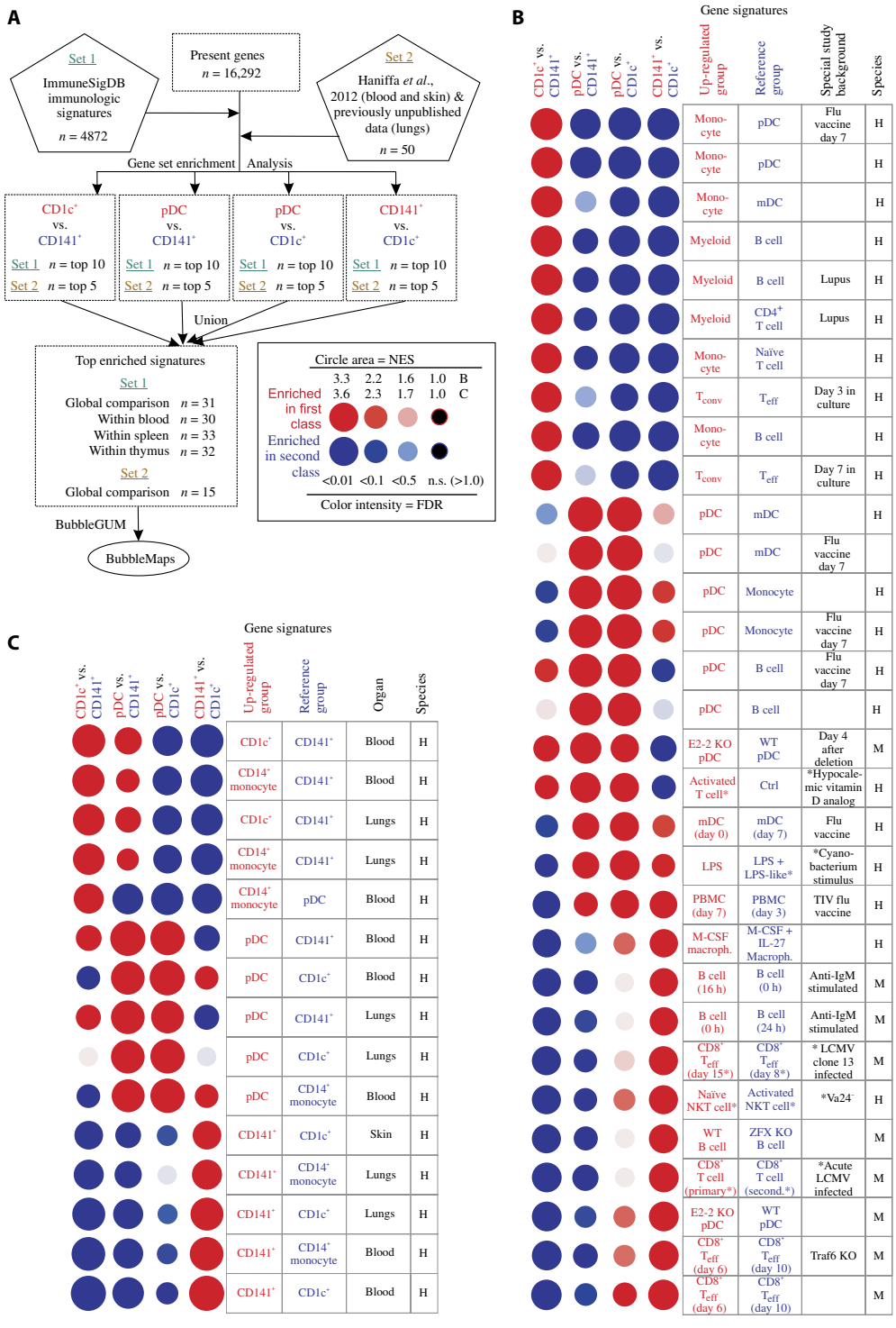

Fig. 8. Mapping ImmuneSigDB signatures onto the human DC transcriptomes. (**A**) Workflow for this figure and fig. S8. NES, normalized enrichment score; n.s., not significant; FDR, false discovery rate. (**B** and **C**) BubbleMaps representing enrichments of selected (B) ImmuneSigDB immunologic signatures and (C) signatures of DCs and monocytes obtained by Haniffa *et al.* (*40*) combined with previously unknown data from human lungs comparing the three major DC subsets. The union of the (B) top 10 or (C) top 5 positively enriched signatures of each of the four specified comparisons is displayed. Enrichment values in the first group are shown in red (positive enrichment), whereas enrichment values in the second group are displayed in blue (negative enrichment). Node size correlates with the NES value, and color intensity represents the FDR. Signatures were ordered according to their BubbleMap profiles. An asterisk (*) in columns "Up-regulated group" or "Reference group" indicates a special study background of the cells (for example, specifically treated cells), which is depicted in the column "Special study background." H, human; M, mouse; Macroph., macrophage; KO, knockout; WT, wild type; T_{conv}, conventional T cells; T_{eff}, effector T cells; LPS, lipopolysaccharide; PBMC, peripheral blood mononuclear cell; M-CSF, macrophage colony-stimulating factor; NKT cell, natural killer T cell; IL-27, interleukin-27; LCMV, lymphocytic choriomeningitis virus; TIV, trivalent influenza vaccine.

Reassessing transcriptomic data sets of DC subsets derived from human lung and skin further supported the panel design of markers for the identification of DC subsets in human tissues as proposed here.

Although we used a tight definition of the different DC subsets based on five to six surface markers each, our unbiased bioinformatic analyses revealed a close relationship of the predefined DC subsets, as illustrated by similar expression of several thousand genes. In contrast, the rather small number of 89 transcripts differentially expressed in DC subsets derived from different lymphohematopoietic tissues reflected a minor degree of microenvironmental influence, which will be subject to future analyses. Recently, Watchmaker *et al.* were able to demonstrate that the transcriptional identity of intestinal CD103$^+$SIRPA$^-$ DCs closely resembles the transcriptional identity of blood CD141$^+$ DCs (*50*). This was in stark contrast to intestinal CD103$^+$SIRPA$^+$ DCs, which differed strongly in their transcriptional footprint from blood- or skin-derived CD1c$^+$ DCs. This discrepancy might be either an evolutionary consequence of a functional conservation across organs within the CD141$^+$ DC lineage or a result of unique functional adaptations due to microenvironmental factors within the CD1c$^+$ DC lineage. Other recent studies suggested a precommitment of murine pre-DCs early in the bone marrow before their immigration into the tissues (*26*, *28*, *36*, *67*). These murine studies and recent findings in the human system (*14*, *16*) support our hypothesis that the transcriptional identity and function of human lymphohematopoietic DCs are mainly dictated by ontogeny and not by their tissue microenvironment. We also extended our analysis toward DC subset signature genes in skin- and lung-derived DC populations, which, in contrast, indicated that these cells are significantly influenced by tissue-specific signals. It will be of great interest to further define the links between marker gene expression and cellular function of the DC subsets in different tissue microenvironments.

Distinct phenotypes and transcriptional programs in the DC subpopulations require a differential composition of TRs governing these processes. In the murine system, a number of TRs essential for the differentiation of the three DC subpopulations have been identified. For example, *Irf8*, *Id2*, and *Batf3* have been linked to CD8α$^+$ and CD103$^+$ DCs, whereas *Irf4*, *Relb*, and *Notch2* are critical for the development of CD11b$^+$ DCs, and *E2-2* is involved in the differentiation of pDCs (*10*, *24*, *25*, *27*, *28*, *34*). In contrast, in human DCs, much less is known about the TRs that might regulate DC differentiation and function. By integrating expression itself, differential expression between the DC subsets, binding prediction to subset-associated gene clusters, previous knowledge about TRs in DCs, and a ranking approach, we defined a smaller set of candidate TRs associated with each of the three DC subsets.

In our analyses, we found *CEBPB*, *SPI1*, *RUNX3*, *NFKB*1, and *BHLHE40* to be among the top-ranking TRs in CD1c$^+$ DCs, whereas this subset displayed a diminished expression of *IRF8*, *MEIS1*, *NR5A1*, *TEAD2*, and *NFAT5*. A similar expression profile of murine DC subsets and precursor DC cultures has already been described for *Cebpb*, *Spi1*, *Nfkb1*, *Bhlhe40*, and *Irf8* (*25*, *50*, *68*). Recently, *Batf3* has been defined as a crucial TR for murine CD8α$^+$ and CD103$^+$ DCs, and data demonstrated that it also directs the development of human CD141$^+$ DCs in a humanized mouse model and in in vitro cultures (*16*, *34*, *47*, *69*). Beside the strong presence of *BATF3* in all analyzed CD141$^+$ DCs, we found *TEAD4*, *MYC*, and *TCF7L2* as the top-ranked TRs, whose functional roles still need to be determined. We could further demonstrate the presence of the TRs *ETS1*, *ARID3A*, *FOXM1*, *BCL11A*, and *TCF3* in pDCs. On the basis of published murine studies, *TCF3* and *BCL11A*, both involved in *E2-2*–dependent transcriptional regulation, might also be crucial for the development of human pDCs (*70*). A recent comparison of cultured human pDCs and monocyte-derived DCs by Bornstein *et al.* demonstrated that *IRF8* functions as an epigenetic and fate-determining TR, including a negative influence on *CEBPB* (*71*). Similarly, independent of tissue origin, we found a clear separation of pDCs from CD1c$^+$ and CD141$^+$ DCs, with the first ones highly positive for *IRF8* and the conventional DCs highly positive for *CEBPB* gene family members.

Some functions of murine DCs have also been shown to be governed by the activity of certain TRs, such as *Rel* or *Nfkb*, which are involved in activation of DCs upon interaction of pathogen-associated molecular patterns with Toll-like receptors (*72*). Because we found those TRs especially present in CD1c$^+$ DCs, further studies need to elucidate whether their high degree of expression accounts for a dominant role of CD1c$^+$ DCs in pathogen recognition. Besides their role in the defense against foreign antigens, DCs are also important for the maintenance of peripheral tolerance. In line with this, one of our earlier studies demonstrated the involvement of murine cDC2 DCs in the expansion of regulatory T cells, which was dependent on transforming growth factor–β (TGF-β) signaling (*73*). In the present study, we found *RUNX3* as a main TR in CD1c$^+$ DCs, a factor important for the regulation of the response to TGF-β (*74*). Certainly, the exact function of individual TRs predicted to be associated with DC subset–specific cellular programming, function, and phenotype requires further experimental validation.

To link genome-wide data sets to previous knowledge, numerous approaches, including gene ontology and pathway enrichment analysis, have been proposed and established in the past. A well-defined data-driven approach to linking data sets to previous knowledge is GSEA (*63*). By far, the largest collection of data-defined gene signatures has been provided by MSigDB (*63*), with a very recent extension of ~5000 immune-related signatures [ImmuneSigDB (*65*)]. Although we could demonstrate that pDCs and the more frequent CD1c$^+$ DCs are already reflected in this rich resource, the infrequent CD141$^+$ DCs were not yet present within these signatures, although this cell subset had already been described in the literature. We therefore developed a simple approach that allowed us to quickly test additional gene signatures not yet being part of ImmuneSigDB. Applying 50 additional signatures from murine and human blood-, skin-, or lung-derived DC subsets to our data set corroborated our major observation that the three DC subsets are distinct cellular entities. Further, microenvironmental signals do not seem to change the major transcriptional programs to a comparable extent observed in other myeloid cell populations. Therefore, the extension of our analyses to other cell types (such as Langerhans cells) for the identification of common molecular signatures will be subject to future investigations (*75*). To enrich MSigDB and ImmuneSigDB for such findings, we would suggest a mechanism that allows the integration of external signatures into these important databases (Fig. 8).

The resource that we provide here should encourage and support future research in DC biology. For example, it will be interesting to understand why there is a differential distribution of the three DC subsets in different tissues. Because very distinct functions have been associated with the three cell types (*49*), it will be interesting to address whether different ratios of these cells lead to differential functionality of the complete DC compartment within a given tissue. Furthermore, albeit the responding DC subsets are similar in different tissues, further studies could address whether the migratory capacities differ and, if so, how these differences are encoded in the transcriptome. Similarly, it will also be important to link tissue residency to the transcriptional modules responsible for this function.

Together, we provide a resource of data containing the three major human DC subpopulations in lymphohematopoietic tissues. Moreover, we encourage the community to use our findings when studying human DCs in the context of tissue homeostasis but more importantly during pathophysiological processes in the context of human diseases.

MATERIALS AND METHODS

Tissue preparation

Leukocyte reduction cones were retrieved from anonymous healthy adult donors. Cord blood was obtained from normal childbirth. Bone marrow was received from biopsies applied for the exclusion of lymphoma or leukemia. Thymus samples were retrieved from cardiac surgeries of otherwise healthy children. The sources of spleen or tonsil samples were patients requiring therapeutic splenectomy or tonsillectomy, respectively. All samples were received under local ethical committee approvals (Ethikkommission der Universität Erlangen-Nürnberg), and informed written consents were obtained in accordance with the Declaration of Helsinki.

None of the donors were positive for HIV or hepatitis C virus, and only samples with reconfirmed negative status of tumor, chronic, or immunological diseases were used in this study. For statistical analyses of DC subpopulation frequencies in the various tissues, 235 different samples (with 30 donations from both blood and spleen, 56 donations from thymus, 54 from tonsils, 22 from bone marrow, and 43 from cord blood) have been analyzed (Fig. 1). All analyzed tissues were derived from different human donors.

All tissue samples were freshly isolated, immediately processed, and enzymatically digested in phosphate-buffered saline (PBS), 2% fetal calf serum (Biochrom) or mixed human serum type AB (Lonza), collagenase D (400 U/ml) (Serva), and 100 μg (spleen and tonsil) to 300 μg (thymus) of deoxyribonuclease I (Sigma). Mechanical disruption was conducted using the gentleMACS tissue dissociator (Miltenyi Biotec). The tissue samples were filtered twice. Single-cell suspensions or directly received donations of blood, cord blood, and bone marrow were diluted with RPMI 1640 medium in a 1:1 ratio, followed by gradient centrifugation as described before as a standard procedure for blood preparation. Surface molecule expression and maturation state of DC subpopulations were not influenced by the applied procedures. In particular, CD83, a marker indicating DC activation, was not expressed on any DC population of the investigated and prepared single-cell suspensions, supporting the finding that the specialized tissue preparations did not initiate the maturation of the different DC subsets (table S1B).

Flow cytometry

Eight- to 18-color flow cytometry was performed on single-cell suspensions (5×10^6 to 8×10^6 cells) of freshly prepared or frozen tissue samples. Cells were stained in one to four steps with differently labeled monoclonal antibodies. For the screening of cell surface molecule expression (Lyoplate assay, BD), the unconjugated antibody (or only PBS, 2% human serum as negative control) was applied first, followed by a secondary goat anti-mouse immunoglobulin G (IgG) or goat anti-rat IgG Alexa Fluor 647 antibody, respectively. In a third round, fluorochrome-conjugated antibodies for the discrimination of different cell populations were used in PBS and 2% human serum. 4′,6-Diamidino-2-phenylindole (0.1 μg/ml) was applied for the exclusion of dead cells.

Cell sorting

Cell sorting was conducted from single-cell suspensions. A DC-defining antibody cocktail was applied, as listed in table S2. A total of 10,000 cells from each sample were directly sorted into RPMI and 2% human serum–containing polymerase chain reaction tubes and washed. During and after sorting, the cells were strictly kept on ice. Pellets were subsequently cryopreserved in liquid nitrogen and stored at −80°C for later experiments. All samples were simultaneously processed by Miltenyi Biotec, including RNA preparation, RNA quality control, RNA super amplification, and microarray hybridization (Whole Human Genome Oligo microarray, 8x60K, Agilent). Raw data files were analyzed using Partek Genomics Suite software.

Summary of bioinformatic analyses

An extended description of all bioinformatic analyses is provided in the Supplementary Materials. Briefly, PCA, SOM clustering, CEA, and a coexpression network were used to display the overall structure of the data set containing the three major DC subsets from three different tissues, as well as blood $CD14^+$ monocytes, B cells, and T cells (fig. S2). The same approaches were used to explore the structure of a reduced data set containing the three DC subsets from blood, spleen, and thymus alone (Fig. 2). Working further with the reduced data set only, genes being specifically expressed in a certain cell type ($CD1c^+$ DCs, $CD141^+$ DCs, and pDCs) or organ (blood, spleen, and thymus) or in one of the DC subsets in a particular organ were identified using linear SVR (*60*) (Fig. 3 and fig. S3) or by considering candidates that show high correlations between gene and protein expression (Fig. 4 and fig. S4). On the basis of the gene lists identified by SVR, a coexpression network (*62*) was generated and used to highlight cell type–specific gene clusters (Fig. 5 and fig. S5). Furthermore, from all annotated, present, and highly correlated TRs in the data set (fig. S6), candidates were allocated to a specific cell type if their target genes showed a large overlap with a corresponding gene cluster in Fig. 3 (Fig. 6). To extend the comparison to non-lymphohematopoietic tissues, an additional data set containing DCs from human blood, skin (*40*), and lung was assembled. Using Pearson correlation values (Fig. 7) and Euclidean distances (fig. S7), the similarities between the DC subsets of different tissues were depicted for each data set separately and then compared. Last, using GSEA (*63*) and BubbleGUM (*64*), gene sets from MSigDB (*63*), from ImmuneSigDB (*65*), and from a large data set previously assembled (*40*) combined with previously unpublished data from human lungs were linked to $CD1c^+$ DCs, $CD141^+$ DCs, and pDCs and visualized in the form of BubbleMaps (Fig. 8 and fig. S8).

SUPPLEMENTARY MATERIALS

immunology.sciencemag.org/cgi/content/full/1/6/eaai7677/DC1

Materials and Methods

Fig. S1. Gating strategy for DC subpopulations and monocytes from different human lymphohematopoietic organs.

Fig. S2. Comparative transcriptomic analysis of DCs, monocytes, and T and B cells.

Fig. S3. Marker genes for human lymphohematopoietic DC subsets.

Fig. S4. Cell surface molecule expression of lymphohematopoietic tissue DC subpopulations and monocytes.

Fig. S5. Generation of coexpression networks.

Fig. S6. Overlaying expression information onto the TR network of human DC subpopulations.

Fig. S7. Comparative analyses of different human lymphohematopoietic and non-lymphohematopoietic tissue DC and monocyte transcriptional data sets.

Fig. S8. ImmuneSigDB signatures related to the major DC subpopulations in blood, spleen, and thymus.

Table S1. Frequencies of human lymphohematopoietic DC subpopulations and expression of common DC or monocyte markers.

Table S2. Gating strategy for sorting DC subpopulations, monocytes, and T and B cells.
Table S3. Signature and marker genes for human lymphohematopoietic DC subsets.
Table S4. Marker genes for the different lymphohematopoietic DC subpopulations.
Table S5. Seven clusters of coexpressed genes.
Table S6. TRs of human lymphohematopoietic DC subpopulations.
Table S7. Similarities between lymphohematopoietic and non-lymphohematopoietic DC subsets.
Table S8. Ranked list of ImmuneSigDB signatures.
References (*76*–*80*)

REFERENCES AND NOTES

1. J. Banchereau, R. M. Steinman, Dendritic cells and the control of immunity. *Nature* **392**, 245–252 (1998).
2. G. F. Heidkamp, C. H. K. Lehmann, L. Heger, A. Baranska, A. Hoffmann, J. Lühr, D. Dudziak, Functional specialization of dendritic cell subsets, in *Encyclopedia of Cell Biology*, P. D. Stahl, Ed. Vol. 3 (Academic Press, 2016), pp. 588–604.
3. R. M. Steinman, J. Banchereau, Taking dendritic cells into medicine. *Nature* **449**, 419–426 (2007).
4. R. M. Steinman, D. Hawiger, M. C. Nussenzweig, Tolerogenic dendritic cells. *Annu. Rev. Immunol.* **21**, 685–711 (2003).
5. D. Dudziak, A. O. Kamphorst, G. F. Heidkamp, V. R. Buchholz, C. Trumpfheller, S. Yamazaki, C. Cheong, K. Liu, H.-W. Lee, C. G. Park, R. M. Steinman, M. C. Nussenzweig, Differential antigen processing by dendritic cell subsets in vivo. *Science* **315**, 107–111 (2007).
6. F. Geissmann, M. G. Manz, S. Jung, M. H. Sieweke, M. Merad, K. Ley, Development of monocytes, macrophages, and dendritic cells. *Science* **327**, 656–661 (2010).
7. K. Liu, G. D. Victora, T. A. Schwickert, P. Guermonprez, M. M. Meredith, K. Yao, F.-F. Chu, G. J. Randolph, A. Y. Rudensky, M. Nussenzweig, In vivo analysis of dendritic cell development and homeostasis. *Science* **324**, 392–397 (2009).
8. K. Liu, C. Waskow, X. Liu, K. Yao, J. Hoh, M. Nussenzweig, Origin of dendritic cells in peripheral lymphoid organs of mice. *Nat. Immunol.* **8**, 578–583 (2007).
9. M. Merad, P. Sathe, J. Helft, J. Miller, A. Mortha, The dendritic cell lineage: Ontogeny and function of dendritic cells and their subsets in the steady state and the inflamed setting. *Annu. Rev. Immunol.* **31**, 563–604 (2013).
10. J. C. Miller, B. D. Brown, T. Shay, E. L. Gautier, V. Jojic, A. Cohain, G. Pandey, M. Leboeuf, K. G. Elpek, J. Helft, D. Hashimoto, A. Chow, J. Price, M. Greter, M. Bogunovic, A. Bellemare-Pelletier, P. S. Frenette, G. J. Randolph, S. J. Turley, M. Merad; Immunological Genome Consortium, Deciphering the transcriptional network of the dendritic cell lineage. *Nat. Immunol.* **13**, 888–899 (2012).
11. S. H. Naik, P. Sathe, H.-Y. Park, D. Metcalf, A. I. Proietto, A. Dakic, S. Carotta, M. O'Keeffe, M. Bahlo, A. Papenfuss, J.-Y. Kwak, L. Wu, K. Shortman, Development of plasmacytoid and conventional dendritic cell subtypes from single precursor cells derived in vitro and in vivo. *Nat. Immunol.* **8**, 1217–1226 (2007).
12. C. Waskow, K. Liu, G. Darrasse-Jèze, P. Guermonprez, F. Ginhoux, M. Merad, T. Shengelia, K. Yao, M. Nussenzweig, The receptor tyrosine kinase Flt3 is required for dendritic cell development in peripheral lymphoid tissues. *Nat. Immunol.* **9**, 676–683 (2008).
13. A. Schlitzer, F. Ginhoux, Organization of the mouse and human DC network. *Curr. Opin. Immunol.* **26**, 90–99 (2014).
14. G. Breton, J. Lee, Y. J. Zhou, J. J. Schreiber, T. Keler, S. Puhr, N. Anandasabapathy, S. Schlesinger, M. Caskey, K. Liu, M. C. Nussenzweig, Circulating precursors of human CD1c$^+$ and CD141$^+$ dendritic cells. *J. Exp. Med.* **212**, 401–413 (2015).
15. M. Guilliams, F. Ginhoux, C. Jakubzick, S. H. Naik, N. Onai, B. U. Schraml, E. Segura, R. Tussiwand, S. Yona, Dendritic cells, monocytes and macrophages: A unified nomenclature based on ontogeny. *Nat. Rev. Immunol.* **14**, 571–578 (2014).
16. J. Lee, G. Breton, T. Y. K. Oliveira, Y. J. Zhou, A. Aljoufi, S. Puhr, M. J. Cameron, R.-P. Sékaly, M. C. Nussenzweig, K. Liu, Restricted dendritic cell and monocyte progenitors in human cord blood and bone marrow. *J. Exp. Med.* **212**, 385–399 (2015).
17. S. Bedoui, P. G. Whitney, J. Waithman, L. Eidsmo, L. Wakim, I. Caminschi, R. S. Allan, M. Wojtasiak, K. Shortman, F. R. Carbone, A. G. Brooks, W. R. Heath, Cross-presentation of viral and self antigens by skin-derived CD103$^+$ dendritic cells. *Nat. Immunol.* **10**, 488–495 (2009).
18. S. Burgdorf, A. Kautz, V. Böhnert, P. A. Knolle, C. Kurts, Distinct pathways of antigen uptake and intracellular routing in CD4 and CD8 T cell activation. *Science* **316**, 612–616 (2007).
19. J. M. M. den Haan, M. J. Bevan, Constitutive versus activation-dependent cross-presentation of immune complexes by CD8$^+$ and CD8$^-$ dendritic cells in vivo. *J. Exp. Med.* **196**, 817–827 (2002).
20. J. Helft, F. Ginhoux, M. Bogunovic, M. Merad, Origin and functional heterogeneity of non-lymphoid tissue dendritic cells in mice. *Immunol. Rev.* **234**, 55–75 (2010).
21. A. O. Kamphorst, P. Guermonprez, D. Dudziak, M. C. Nussenzweig, Route of antigen uptake differentially impacts presentation by dendritic cells and activated monocytes. *J. Immunol.* **185**, 3426–3435 (2010).
22. J. L. Pooley, W. R. Heath, K. Shortman, Cutting edge: Intravenous soluble antigen is presented to CD4 T cells by CD8$^-$ dendritic cells, but cross-presented to CD8 T cells by CD8$^+$ dendritic cells. *J. Immunol.* **166**, 5327–5330 (2001).
23. D. K. Fogg, C. Sibon, C. Miled, S. Jung, P. Aucouturier, D. R. Littman, A. Cumano, F. Geissmann, A clonogenic bone marrow progenitor specific for macrophages and dendritic cells. *Science* **311**, 83–87 (2006).
24. A. Schlitzer, N. McGovern, P. Teo, T. Zelante, K. Atarashi, D. Low, A. W. S. Ho, P. See, A. Shin, P. S. Wasan, G. Hoeffel, B. Malleret, A. Heiseke, S. Chew, L. Jardine, H. A. Purvis, C. M. U. Hilkens, J. Tam, M. Poidinger, E. R. Stanley, A. B. Krug, L. Renia, B. Sivasankar, L. G. Ng, M. Collin, P. Ricciardi-Castagnoli, K. Honda, M. Haniffa, F. Ginhoux, IRF4 transcription factor-dependent CD11b$^+$ dendritic cells in human and mouse control mucosal IL-17 cytokine responses. *Immunity* **38**, 970–983 (2013).
25. G. T. Belz, S. L. Nutt, Transcriptional programming of the dendritic cell network. *Nat. Rev. Immunol.* **12**, 101–113 (2012).
26. F. Paul, Y. Arkin, A. Giladi, D. A. Jaitin, E. Kenigsberg, H. Keren-Shaul, D. Winter, D. Lara-Astiaso, M. Gury, A. Weiner, E. David, N. Cohen, F. K. Lauridsen, S. Haas, A. Schlitzer, A. Mildner, F. Ginhoux, S. Jung, A. Trumpp, B. T. Porse, A. Tanay, I. Amit, Transcriptional heterogeneity and lineage commitment in myeloid progenitors. *Cell* **163**, 1663–1677 (2015).
27. B. Reizis, A. Bunin, H. S. Ghosh, K. L. Lewis, V. Sisirak, Plasmacytoid dendritic cells: Recent progress and open questions. *Annu. Rev. Immunol.* **29**, 163–183 (2011).
28. A. Schlitzer, V. Sivakamasundari, J. Chen, H. R. B. Sumatoh, J. Schreuder, J. Lum, B. Malleret, S. Zhang, A. Larbi, F. Zolezzi, L. Renia, M. Poidinger, S. Naik, E. W. Newell, P. Robson, F. Ginhoux, Identification of cDC1- and cDC2-committed DC progenitors reveals early lineage priming at the common DC progenitor stage in the bone marrow. *Nat. Immunol.* **16**, 718–728 (2015).
29. M. Swiecki, M. Colonna, The multifaceted biology of plasmacytoid dendritic cells. *Nat. Rev. Immunol.* **15**, 471–485 (2015).
30. E. K. Persson, H. Uronen-Hansson, M. Semmrich, A. Rivollier, K. Hägerbrand, J. Marsal, S. Gudjonsson, U. Håkansson, B. Reizis, K. Kotarsky, W. W. Agace, IRF4 transcription-factor-dependent CD103$^+$CD11b$^+$ dendritic cells drive mucosal T helper 17 cell differentiation. *Immunity* **38**, 958–969 (2013).
31. M. M. Meredith, K. Liu, G. Darrasse-Jeze, A. O. Kamphorst, H. A. Schreiber, P. Guermonprez, J. Idoyaga, C. Cheong, K.-H. Yao, R. E. Niec, M. C. Nussenzweig, Expression of the zinc finger transcription factor zDC (Zbtb46, Btbd4) defines the classical dendritic cell lineage. *J. Exp. Med.* **209**, 1153–1165 (2012).
32. K. L. Lewis, M. L. Caton, M. Bogunovic, M. Greter, L. T. Grajkowska, D. Ng, A. Klinakis, I. F. Charo, S. Jung, J. L. Gommerman, I. I. Ivanov, K. Liu, M. Merad, B. Reizis, Notch2 receptor signaling controls functional differentiation of dendritic cells in the spleen and intestine. *Immunity* **35**, 780–791 (2011).
33. F. Ginhoux, K. Liu, J. Helft, M. Bogunovic, M. Greter, D. Hashimoto, J. Price, N. Yin, J. Bromberg, S. A. Lira, E. R. Stanley, M. Nussenzweig, M. Merad, The origin and development of nonlymphoid tissue CD103$^+$ DCs. *J. Exp. Med.* **206**, 3115–3130 (2009).
34. K. Hildner, B. T. Edelson, W. E. Purtha, M. Diamond, H. Matsushita, M. Kohyama, B. Calderon, B. U. Schraml, E. R. Unanue, M. S. Diamond, R. D. Schreiber, T. L. Murphy, K. M. Murphy, *Batf3* deficiency reveals a critical role for CD8α^+ dendritic cells in cytotoxic T cell immunity. *Science* **322**, 1097–1100 (2008).
35. B. Cisse, M. L. Caton, M. Lehner, T. Maeda, S. Scheu, R. Locksley, D. Holmberg, C. Zweier, N. S. den Hollander, S. G. Kant, W. Holter, A. Rauch, Y. Zhuang, B. Reizis, Transcription factor E2-2 is an essential and specific regulator of plasmacytoid dendritic cell development. *Cell* **135**, 37–48 (2008).
36. G. E. Grajales-Reyes, A. Iwata, J. Albring, X. Wu, R. Tussiwand, W. KC, N. M. Kretzer, C. G. Briseño, V. Durai, P. Bagadia, M. Haldar, J. Schönheit, F. Rosenbauer, T. L. Murphy, K. M. Murphy, Batf3 maintains autoactivation of *Irf8* for commitment of a CD8α^+ conventional DC clonogenic progenitor. *Nat. Immunol.* **16**, 708–717 (2015).
37. R. Tussiwand, B. Everts, G. E. Grajales-Reyes, N. M. Kretzer, A. Iwata, J. Bagaitkar, X. Wu, R. Wong, D. A. Anderson, T. L. Murphy, E. J. Pearce, K. M. Murphy, *Klf4* expression in conventional dendritic cells is required for T helper 2 cell responses. *Immunity* **42**, 916–928 (2015).
38. T. Yi, J. G. Cyster, EBI2-mediated bridging channel positioning supports splenic dendritic cell homeostasis and particulate antigen capture. *eLife* **2**, e00757 (2013).
39. L. Wu, A. D'Amico, K. D. Winkel, M. Suter, D. Lo, K. Shortman, RelB is essential for the development of myeloid-related CD8α^- dendritic cells but not of lymphoid-related CD8α^+ dendritic cells. *Immunity* **9**, 839–847 (1998).
40. M. Haniffa, A. Shin, V. Bigley, N. McGovern, P. Teo, P. See, P. S. Wasan, X.-N. Wang, F. Malinarich, B. Malleret, A. Larbi, P. Tan, H. Zhao, M. Poidinger, S. Pagan, S. Cookson, R. Dickinson, I. Dimmick, R. F. Jarrett, L. Renia, J. Tam, C. Song, J. Connolly, J. K. Y. Chan, A. Gehring, A. Bertoletti, M. Collin, F. Ginhoux, Human tissues contain CD141^{hi} cross-presenting dendritic cells with functional homology to mouse CD103$^+$ nonlymphoid dendritic cells. *Immunity* **37**, 60–73 (2012).

41. E. Segura, J. Valladeau-Guilemond, M.-H. Donnadieu, X. Sastre-Garau, V. Soumelis, S. Amigorena, Characterization of resident and migratory dendritic cells in human lymph nodes. *J. Exp. Med.* **209**, 653–660 (2012).
42. A. Bachem, S. Güttler, E. Hartung, F. Ebstein, M. Schaefer, A. Tannert, A. Salama, K. Movassaghi, C. Opitz, H. W. Mages, V. Henn, P.-M. Kloetzel, S. Gurka, R. A. Kroczek, Superior antigen cross-presentation and XCR1 expression define human CD11c$^+$CD141$^+$ cells as homologues of mouse CD8$^+$ dendritic cells. *J. Exp. Med.* **207**, 1273–1281 (2010).
43. K. Crozat, R. Guiton, V. Contreras, V. Feuillet, C.-A. Dutertre, E. Ventre, T.-P. V. Manh, T. Baranek, A. K. Storset, J. Marvel, P. Boudinot, A. Hosmalin, I. Schwartz-Cornil, M. Dalod, The XC chemokine receptor 1 is a conserved selective marker of mammalian cells homologous to mouse CD8α^+ dendritic cells. *J. Exp. Med.* **207**, 1283–1292 (2010).
44. A. Dzionek, A. Fuchs, P. Schmidt, S. Cremer, M. Zysk, S. Miltenyi, D. W. Buck, J. Schmitz, BDCA-2, BDCA-3, and BDCA-4: Three markers for distinct subsets of dendritic cells in human peripheral blood. *J. Immunol.* **165**, 6037–6046 (2000).
45. A. Dzionek, Y. Sohma, J. Nagafune, M. Cella, M. Colonna, F. Facchetti, G. Günther, I. Johnston, A. Lanzavecchia, T. Nagasaka, T. Okada, W. Vermi, G. Winkels, T. Yamamoto, M. Zysk, Y. Yamaguchi, J. Schmitz, BDCA-2, a novel plasmacytoid dendritic cell–specific type II C-type lectin, mediates antigen capture and is a potent inhibitor of interferon α/β induction. *J. Exp. Med.* **194**, 1823–1834 (2001).
46. S. L. Jongbloed, A. J. Kassianos, K. J. McDonald, G. J. Clark, X. Ju, C. E. Angel, C.-J. J. Chen, P. R. Dunbar, R. B. Wadley, V. Jeet, A. J. E. Vulink, D. N. J. Hart, K. J. Radford, Human CD141$^+$ (BDCA-3)$^+$ dendritic cells (DCs) represent a unique myeloid DC subset that cross-presents necrotic cell antigens. *J. Exp. Med.* **207**, 1247–1260 (2010).
47. L. F. Poulin, M. Salio, E. Griessinger, F. Anjos-Afonso, L. Craciun, J.-L. Chen, A. M. Keller, O. Joffre, S. Zelenay, E. Nye, A. Le Moine, F. Faure, V. Donckier, D. Sancho, V. Cerundolo, D. Bonnet, C. Reis e Sousa, Characterization of human DNGR-1$^+$ BDCA3$^+$ leukocytes as putative equivalents of mouse CD8α^+ dendritic cells. *J. Exp. Med.* **207**, 1261–1271 (2010).
48. S. H. Robbins, T. Walzer, D. Dembélé, C. Thibault, A. Defays, G. Bessou, H. Xu, E. Vivier, M. Sellars, P. Pierre, F. R. Sharp, S. Chan, P. Kastner, M. Dalod, Novel insights into the relationships between dendritic cell subsets in human and mouse revealed by genome-wide expression profiling. *Genome Biol.* **9**, R17 (2008).
49. E. Segura, M. Durand, S. Amigorena, Similar antigen cross-presentation capacity and phagocytic functions in all freshly isolated human lymphoid organ–resident dendritic cells. *J. Exp. Med.* **210**, 1035–1047 (2013).
50. P. B. Watchmaker, K. Lahl, M. Lee, D. Baumjohann, J. Morton, S. J. Kim, R. Zeng, A. Dent, K. M. Ansel, B. Diamond, H. Hadeiba, E. C. Butcher, Comparative transcriptional and functional profiling defines conserved programs of intestinal DC differentiation in humans and mice. *Nat. Immunol.* **15**, 98–108 (2014).
51. M. Colonna, G. Trinchieri, Y.-J. Liu, Plasmacytoid dendritic cells in immunity. *Nat. Immunol.* **5**, 1219–1226 (2004).
52. Y.-J. Liu, IPC: Professional type 1 interferon-producing cells and plasmacytoid dendritic cell precursors. *Annu. Rev. Immunol.* **23**, 275–306 (2005).
53. N. Kolesnikov, E. Hastings, M. Keays, O. Melnichuk, Y. A. Tang, E. Williams, M. Dylag, N. Kurbatova, M. Brandizi, T. Burdett, K. Megy, E. Pilicheva, G. Rustici, A. Tikhonov, H. Parkinson, R. Petryszak, U. Sarkans, A. Brazma, ArrayExpress update—Simplifying data submissions. *Nucleic Acids Res.* **43**, D1113–D1116 (2015).
54. M. Lindstedt, K. Lundberg, C. A. K. Borrebaeck, Gene family clustering identifies functionally associated subsets of human in vivo blood and tonsillar dendritic cells. *J. Immunol.* **175**, 4839–4846 (2005).
55. K. Lundberg, A.-S. Albrekt, I. Nelissen, S. Santegoets, T. D. de Gruijl, S. Gibbs, M. Lindstedt, Transcriptional profiling of human dendritic cell populations and models - unique profiles of in vitro dendritic cells and implications on functionality and applicability. *PLOS ONE* **8**, e52875 (2013).
56. E. Segura, M. Touzot, A. Bohineust, A. Cappuccio, G. Chiocchia, A. Hosmalin, M. Dalod, V. Soumelis, S. Amigorena, Human inflammatory dendritic cells induce Th17 cell differentiation. *Immunity* **38**, 336–348 (2013).
57. F. Ginhoux, J. L. Schultze, P. J. Murray, J. Ochando, S. K. Biswas, New insights into the multidimensional concept of macrophage ontogeny, activation and function. *Nat. Immunol.* **17**, 34–40 (2016).
58. Y. Lavin, D. Winter, R. Blecher-Gonen, E. David, H. Keren-Shaul, M. Merad, S. Jung, I. Amit, Tissue-resident macrophage enhancer landscapes are shaped by the local microenvironment. *Cell* **159**, 1312–1326 (2014).
59. J. Xue, S. V. Schmidt, J. Sander, A. Draffehn, W. Krebs, I. Quester, D. De Nardo, T. D. Gohel, M. Emde, L. Schmidleithner, H. Ganesan, A. Nino-Castro, M. R. Mallmann, L. Labzin, H. Theis, M. Kraut, M. Beyer, E. Latz, T. C. Freeman, T. Ulas, J. L. Schultze, Transcriptome-based network analysis reveals a spectrum model of human macrophage activation. *Immunity* **40**, 274–288 (2014).
60. A. M. Newman, C. L. Liu, M. R. Green, A. J. Gentles, W. Feng, Y. Xu, C. D. Hoang, M. Diehn, A. A. Alizadeh, Robust enumeration of cell subsets from tissue expression profiles. *Nat. Methods* **12**, 453–457 (2015).
61. K. Bratke, J. Nielsen, F. Manig, C. Klein, M. Kuepper, S. Geyer, P. Julius, M. Lommatzsch, J. C. Virchow, Functional expression of granzyme B in human plasmacytoid dendritic cells: A role in allergic inflammation. *Clin. Exp. Allergy* **40**, 1015–1024 (2010).
62. A. Theocharidis, S. van Dongen, A. J. Enright, T. C. Freeman, Network visualization and analysis of gene expression data using BioLayout *Express*^{3D}. *Nat. Protoc.* **4**, 1535–1550 (2009).
63. A. Subramanian, P. Tamayo, V. K. Mootha, S. Mukherjee, B. L. Ebert, M. A. Gillette, A. Paulovich, S. L. Pomeroy, T. R. Golub, E. S. Lander, J. P. Mesirov, Gene set enrichment analysis: A knowledge-based approach for interpreting genome-wide expression profiles. *Proc. Natl. Acad. Sci. U.S.A.* **102**, 15545–15550 (2005).
64. L. Spinelli, S. Carpentier, F. Montañana Sanchis, M. Dalod, T.-P. V. Manh, BubbleGUM: Automatic extraction of phenotype molecular signatures and comprehensive visualization of multiple Gene Set Enrichment Analyses. *BMC Genomics* **16**, 814 (2015).
65. J. Godec, Y. Tan, A. Liberzon, P. Tamayo, S. Bhattacharya, A. J. Butte, J. P. Mesirov, W. N. Haining, Compendium of immune signatures identifies conserved and species-specific biology in response to inflammation. *Immunity* **44**, 194–206 (2016).
66. E. Klechevsky, Functional diversity of human dendritic cells. *Adv. Exp. Med. Biol.* **850**, 43–54 (2015).
67. S. H. Naik, L. Perié, E. Swart, C. Gerlach, N. van Rooij, R. J. de Boer, T. N. Schumacher, Diverse and heritable lineage imprinting of early haematopoietic progenitors. *Nature* **496**, 229–232 (2013).
68. P. Felker, K. Seré, Q. Lin, C. Becker, M. Hristov, T. Hieronymus, M. Zenke, TGF-β1 accelerates dendritic cell differentiation from common dendritic cell progenitors and directs subset specification toward conventional dendritic cells. *J. Immunol.* **185**, 5326–5335 (2010).
69. L. F. Poulin, Y. Reyal, H. Uronen-Hansson, B. U. Schraml, D. Sancho, K. M. Murphy, U. K. Håkansson, L. F. Moita, W. W. Agace, D. Bonnet, C. Reis e Sousa, DNGR-1 is a specific and universal marker of mouse and human Batf3-dependent dendritic cells in lymphoid and nonlymphoid tissues. *Blood* **119**, 6052–6062 (2012).
70. G. C. Ippolito, J. D. Dekker, Y.-H. Wang, B.-K. Lee, A. L. Shaffer III, J. Lin, J. K. Wall, B.-S. Lee, L. M. Staudt, Y.-J. Liu, V. R. Iyer, H. O. Tucker, Dendritic cell fate is determined by BCL11A. *Proc. Natl. Acad. Sci. U.S.A.* **111**, E998–E1006 (2014).
71. C. Bornstein, D. Winter, Z. Barnett-Itzhaki, E. David, S. Kadri, M. Garber, I. Amit, A negative feedback loop of transcription factors specifies alternative dendritic cell chromatin states. *Mol. Cell* **56**, 749–762 (2014).
72. O. Takeuchi, S. Akira, Pattern recognition receptors and inflammation. *Cell* **140**, 805–820 (2010).
73. S. Yamazaki, D. Dudziak, G. F. Heidkamp, C. Fiorese, A. J. Bonito, K. Inaba, M. C. Nussenzweig, R. M. Steinman, CD8$^+$ CD205$^+$ splenic dendritic cells are specialized to induce Foxp3$^+$ regulatory T cells. *J. Immunol.* **181**, 6923–6933 (2008).
74. O. Fainaru, E. Woolf, J. Lotem, M. Yarmus, O. Brenner, D. Goldenberg, V. Negreanu, Y. Bernstein, D. Levanon, S. Jung, Y. Groner, Runx3 regulates mouse TGF-β-mediated dendritic cell function and its absence results in airway inflammation. *EMBO J.* **23**, 969–979 (2004).
75. S. Carpentier, T.-P. V. Manh, R. Chelbi, S. Henri, B. Malissen, M. Haniffa, F. Ginhoux, M. Dalod, Comparative genomics analysis of mononuclear phagocyte subsets confirms homology between lymphoid tissue-resident and dermal XCR1$^+$ DCs in mouse and human and distinguishes them from Langerhans cells. *J. Immunol. Methods* **432**, 35–49 (2016).
76. P. Shannon, A. Markiel, O. Ozier, N. S. Baliga, J. T. Wang, D. Ramage, N. Amin, B. Schwikowski, T. Ideker, Cytoscape: A software environment for integrated models of biomolecular interaction networks. *Genome Res.* **13**, 2498–2504 (2003).
77. M. B. Gerstein, A. Kundaje, M. Hariharan, S. G. Landt, K.-K. Yan, C. Cheng, X. J. Mu, E. Khurana, J. Rozowsky, R. Alexander, R. Min, P. Alves, A. Abyzov, N. Addleman, N. Bhardwaj, A. P. Boyle, P. Cayting, A. Charos, D. Z. Chen, Y. Cheng, D. Clarke, C. Eastman, G. Euskirchen, S. Frietze, Y. Fu, J. Gertz, F. Grubert, A. Harmanci, P. Jain, M. Kasowski, P. Lacroute, J. Leng, J. Lian, H. Monahan, H. O'Geen, Z. Ouyang, E. C. Partridge, D. Patacsil, F. Pauli, D. Raha, L. Ramirez, T. E. Reddy, B. Reed, M. Shi, T. Slifer, J. Wang, L. Wu, X. Yang, K. Y. Yip, G. Zilberman-Schapira, S. Batzoglou, A. Sidow, P. J. Farnham, R. M. Myers, S. M. Weissman, M. Snyder, Architecture of the human regulatory network derived from ENCODE data. *Nature* **489**, 91–100 (2012).
78. J. Wang, J. Zhuang, S. Iyer, X.-Y. Lin, M. C. Greven, B.-H. Kim, J. Moore, B. G. Pierce, X. Dong, D. Virgil, E. Birney, J.-H. Hung, Z. Weng, Factorbook.org: A Wiki-based database for transcription factor-binding data generated by the ENCODE consortium. *Nucleic Acids Res.* **41**, D171–D176 (2013).
79. F. Zhao, Z. Xuan, L. Liu, M. Q. Zhang, TRED: A Transcriptional Regulatory Element Database and a platform for in silico gene regulation studies. *Nucleic Acids Res.* **33**, D103–D107 (2005).
80. G. Zheng, K. Tu, Q. Yang, Y. Xiong, C. Wei, L. Xie, Y. Zhu, Y. Li, ITFP: An integrated platform of mammalian transcription factors. *Bioinformatics* **24**, 2416–2417 (2008).

Acknowledgments: We thank S. Beck and C. Weiss for technical support. We are grateful for cell-sorting support especially by M. Mroz and D. Schönhöfer (Core Unit Cell Sorting and Immunomonitoring) as well as the support by the Medical Immunology Campus Erlangen (MICE) and the Optical Imaging Center Erlangen (OICE). We thank M. Teichmann and R.-M. Zippel from the Department of Hematology and Medical Oncology at the Sozialstiftung Bamberg for human tissue sample supply. We also thank the members of the Dudziak and Nimmerjahn laboratories for their critical comments. Parts of this work were leading to the initiation of a FAU (Friedrich-Alexander University Erlangen-Nürnberg) Emerging Fields Initiative BIG-Thera (D.D., P.A.F., F.N., and C.A.). **Funding:** This work was partly supported by grants from the German Research Foundation [Deutsche Forschungsgemeinschaft (DFG)] to D.D. (DU548/2-1, Emmy Noether Programme, CRC643-TPA7, CRC1181-TPA7, RTG1962, and RTG1660), F.N. (CRC643-TPA8, CRC643-TPB14, and CRC1181-TPA7), C.A. (DFG SPP 1681), A.S. (Emmy Noether Programme SCHL 2116/1-1), and J.L.S. (CRC645 and CRC704). E.U. was funded by the LOEWE Center for Cell and Gene Therapy (Hessian Ministry of Higher Education, Research and the Arts, III L 4- 518/17.004). G.F.H. was supported by Erlanger Leistungsbezogene Anschubfinanzierung und Nachwuchsförderung (ELAN) (DE-14-10-17-1-Heidkamp). C.H.K.L., F.N., and D.D. received support from Interdisziplinäres Zentrum für Klinische Forschung (IZKF) (IZKF-J54, IZKF-A65, and IZKF-A68). D.D. and F.N. were both supported by BayGene. D.D. was a fellow of the "Young Colleague" of the Bavarian Academy of Sciences. A.S. and J.L.S. are members of the Excellence Cluster ImmunoSensation. **Author contributions:** G.F.H. performed the experiments. J.S. analyzed data. C.H.K.L., T.U., A.L., and F.N. contributed to data analysis and interpretation as well as discussions. L.H., N.E., A.B., J.J.L., N.M., F.G., A.S., A. Hoffmann, and K.C.R. participated in performing the experiments and contributed to the review of the manuscript. S.S., A. Hartmann, J.Z., C.A., B. Spriewald, A.M., G.S., B. Schauf, A.F., R.R., P.A.F., A.P., R.C., F.G., and E.U. ensured human tissue sample supply. J.L.S. and D.D. wrote the manuscript. **Competing interests:** The authors declare that they have no conflicting financial interests. **Data and materials availability:** All microarray data are available in the Gene Expression Omnibus database (www.ncbi.nlm.nih.gov/gds) under the accession numbers GSE77671, GSE85305, and GSE87494.

Submitted 9 August 2016
Accepted 14 November 2016
Published 16 December 2016
10.1126/sciimmunol.aai7677

Citation: G. F. Heidkamp, J. Sander, C. H. K. Lehmann, L. Heger, N. Eissing, A. Baranska, J. J. Lühr, A. Hoffmann, K. C. Reimer, A. Lux, S. Söder, A. Hartmann, J. Zenk, T. Ulas, N. McGovern, C. Alexiou, B. Spriewald, A. Mackensen, G. Schuler, B. Schauf, A. Forster, R. Repp, P. A. Fasching, A. Purbojo, R. Cesnjevar, E. Ullrich, F. Ginhoux, A. Schlitzer, F. Nimmerjahn, J. L. Schultze, D. Dudziak, Human lymphoid organ dendritic cell identity is predominantly dictated by ontogeny, not tissue microenvironment. *Sci. Immunol.* **1**, eaai7677 (2016).

Science Immunology
AAAS

Human lymphoid organ dendritic cell identity is predominantly dictated by ontogeny, not tissue microenvironment

Gordon F. Heidkamp, Jil Sander, Christian H. K. Lehmann, Lukas Heger, Nathalie Eissing, Anna Baranska, Jennifer J. Lühr, Alana Hoffmann, Katharina C. Reimer, Anja Lux, Stephan Söder, Arndt Hartmann, Johannes Zenk, Thomas Ulas, Naomi McGovern, Christoph Alexiou, Bernd Spriewald, Andreas Mackensen, Gerold Schuler, Burkhard Schauf, Anja Forster, Roland Repp, Peter A. Fasching, Ariawan Purbojo, Robert Cesnjevar, Evelyn Ullrich, Florent Ginhoux, Andreas Schlitzer, Falk Nimmerjahn, Joachim L. Schultze and Diana Dudziak

*Sci. Immunol.*1, (2016)
doi: 10.1126/sciimmunol.aai7677

Editor's Summary Dendritic cell branchesDendritic cell (DC) subsets have been well studied in mice; however, the relative contribution of ontogeny and tissue microenvironment to DC function in humans is less clear. Now, Heidkamp et al. perform phenotypic and transcriptional profiling of three DC subtypes in different human tissues from a large number of individuals. They find that DC subpopulations in more lympho-hemaotopoietic organs (spleen, thymus, and blood) are more strongly influenced by ontogeny, whereas those from lung and skin may be influenced by the issue microenvironment. The data collected here provide an in depth look at the transcriptional profile of dendritic cell subsets in humans and inform our understanding of human DC biology.